8-2007

SIMULATION OF A BACKREST MOMENT TEST FOR AN AUTOMOTIVE FRONT SEAT USING NONLINEAR CONTACT FINITE ELEMENT ANALYSIS

Abhinand Chelikani
Clemson University, achelik@clemson.edu

SIMULATION OF A BACKREST MOMENT TEST FOR AN AUTOMOTIVE FRONT SEAT USING NONLINEAR CONTACT FINITE ELEMENT ANALYSIS

A Thesis
Presented to
the Graduate School of
Clemson University

In Partial Fulfillment
of the Requirements for the Degree
Master of Science
Mechanical Engineering

---

by
Abhinand Chelikani
August 2007

Accepted by:
Dr. Lonny L. Thompson, Committee Chair
Dr. Sherrill B.Biggers
Dr. Adralan Vahidi

ABSTRACT

Computer aided engineering and finite element simulation are essential in order to predict accurately the safety performance of automotive structures in an event of crash. In this work, finite element simulation is used to evaluate the strength and deflection characteristics of a reference automotive front seat in an event of vehicle rear impact. Understanding the strength-deflection characteristics of front automotive seats during vehicle rear impact is important to ensure the safety function of the seat. The safety function is measured based on a moment test in accordance with government (ECE R17) regulations. Accurate finite element modeling of a reference seat which has passed ECE R17 moment test requirements is important to provide a benchmark reference to compare new concepts and designs which reduce weight while maintaining minimum test requirements.

In this work, simulation of the moment test of the reference seat is done beyond the component level by using a complete seat model formed by integrating the major structural components including the base frame, slider rails and backrest. The stamped sheet metal structural frames are represented in the finite element using shell elements. Contact within the seat structure is defined in order to simulate joints between side flanges and cross tube members of the base frame. Contact modeling is also used to simulate the interaction of a SAE J826 rigid body form with the backrest. Height adjustment, front tilt adjustment and the backrest tilt angle adjustment locking mechanisms are represented in the finite element model using rigid connections. The bolt connections between different parts in the model are represented using multi-point constraints. An elastic-plastic material is used to model the ductile steel structures. Different grades of steel with low, medium, and high ultimate strength are considered for the different components. In order to confirm the strength requirements, moment deflection characteristics of the seat are studied in accordance with ECE R17. The strength and deflection

characteristics of the seat are obtained by simulating the quasi-static moment test in ABAQUS/Explicit using two complementary loading cases, constant horizontal force and constant angular velocity. For the moment test, simulated using constant horizontal force, the results show that the seat satisfies a maximum moment requirement and, at the end of the deformation travel, the developed moment is maintained above a minimum requirement. For the moment test simulated using the constant angular velocity, the maximum moment is not reached, yet after the end of deformation travel, the developed moment stays above the minimum.

Since the ECE R17 regulations do not provide precise specifications for the height of the applied force and test setup for the body form pivot mechanism, a study is conducted in order to understand the influence of body form rotation and height of the body form above the H-point, representing the physical pivot of the occupant hip area. The influence of plastic material properties of different grades of steel used for the seat model, front mesh contour on the backrest and connection between the backrest and connector are also modified to analyze the influence of load path on moment deflection characteristics of a seat. The moment test setup with increased distance of 430 mm between H-point and reference point of the body form shows higher strength for initial deflection and lower strength towards the end of the deformation path when compared to original length of 360mm. The moment test setup with body rotation about the reference point axis constrained shows higher strength for initial deflection and similar strength towards the end of the deformation path when compared to free rotation of the body form reference point axis. The front mesh without contour on the backrest decreases the strength of the seat below the requirement. Changing the ultimate strength of steel used on the major load bearing components does change the component stress, but shows only a small change in the moment deflection characteristics of the model. Using a high yield strength steel material for the connector increases the maximum moment that the seat can support.

DEDICATION

This thesis is dedicated to my parents Surya Rao and Padma Chelikani.

ACKNOWLEDGEMENTS

First and foremost, I offer my sincerest gratitude to my research advisor, Dr Lonny L. Thompson, who has supported me throughout my thesis and BMW lightweight engineering project with his patience and knowledge. I attribute the level of my Masters degree to his encouragement and effort without which this thesis would not have been completed. I would like to thank my committee members, Dr. Sherrill Biggers and Dr. Ardalan Vahidi, for their suggestions regarding my thesis. I would also like to thank Mr. Norbert Seyr for his many contributions and to BMW for funding this lightweight engineering project.

Furthermore, I would like to thank my BMW lightweight engineering project partner Manoj Kumar Chinnakonda for providing a stimulating and fun environment to learn and grow.

Finally, I would like to thank my parents, Surya Rao and Padma Chelikani for their encouragement and moral support through out my education.

TABLE OF CONTENTS

Page

TABLE OF CONTENTS (Continued)

Page

LIST OF TABLES

Table Page

LIST OF FIGURES

Figure Page

LIST OF FIGURES (Continued)

Figure Page

LIST OF FIGURES (Continued)

Figure Page

LIST OF FIGURES (Continued)

Figure Page

CHAPTER 1

INTRODUCTION

Finite Element Analysis (FEA) is an extremely efficient and economical tool for designing and predicting the performance of structural components in an automobile. FEA is used to guide the design process from conceptual to the detailed stage, see e.g. [1]. The finite element simulations can be used to predict the strength and deformation behavior of models without conducting costly and time consuming physical testing. FEA is also used to validate the design process and help optimize the designed automotive assemblies and components [2].

The increasing functional requirements of safety, comfort, light weight, and other factors for automotive seats have increased the complexity of designing optimized seats. Increased safety requirements to prevent injury during crash events from government regulations have increased the number and severity of strength tests which automotive seats must pass before production. Often both European Union regulations such as ECE R17 [3] and North American regulations such as Federal Motor Vehicle Safety Standards (FMVSS) 202 for seats and their anchorages are required [4]. In addition, automotive Original Equipment Manufacturers (OEM) often exceeds the load requirements of government regulations. The modeling techniques in finite element analysis for accurate prediction are challenged by the complex design of the seating structure when optimized for the often competing requirements of strength for safety, light weight, and comfort functions. Since the safety requirements are based on high speed impact crash tests, automotive seat structures will generally yield under the specified load requirements and thus nonlinear finite element analysis is required, often with surface contact interaction models between parts in assemblies. Most seats have locking adjustment mechanisms for backrest tilt angle, height adjustment, front tilt, slider rail longitudinal adjustments. Accurate, yet efficient finite element models of these locking mechanisms are a challenge for the analyst. Because of the different

functionalities of the seat, different materials are used, for example, Poly Urethane foam for the seating surfaces for comfort, and stamped steel sheet or high-pressure die cast magnesium alloy, and other high strength materials for structural frames.

1.1 Literature Review

In a research project at University of Virginia funded by the NHTSA, a study was conducted in order to identify the safety issues related to rear impact. The strength characteristics of seats from different OEM's were assessed in accordance with FMVSS 202 [5]. The strength deflection characteristics of the automotive front seat are measured using the test procedure SAE J879 in accordance with FMVSS 202 [5]. According to SAE J879 testing procedure, a force is applied on the top cross member of the backrest normal to the torso line. FMVSS 202 [4] requires the seat to with stand a moment of 373 N-m about the H-point [5]. The H-point is located in front of the backrest and above the seat and represents the pivot point of the occupant hip joint. The torso line represents a line through the occupant back. The torso angle is measured from the vertical with respect to ground. The seat is loaded using the head form defined in FMVSS 202 attached to a loading arm rotating about the H-point [5]. The seat is loaded by rotating the body form attached to an arm with an angular displacement of 2 degrees/sec about the H-point. The moment measured is given by the product of force acting normal to the torso line and perpendicular distance between the H-point and point of application of load [3]. The moment deflection characteristics are obtained by plotting the moment calculated against the angular deflection of the seat. The moment test conducted on a Saab 900S driver front seat was found to withstand a maximum moment of 2294 N-m with strength characteristics higher than all the other seats tested. The seat back and recliner mechanism deformed significantly but the recliner locking mechanism still remained engaged [5]. The inspection of seats tested for strength requirements showed that the failure occurred above the recliner mechanism with the backrest tilt lock engaged.

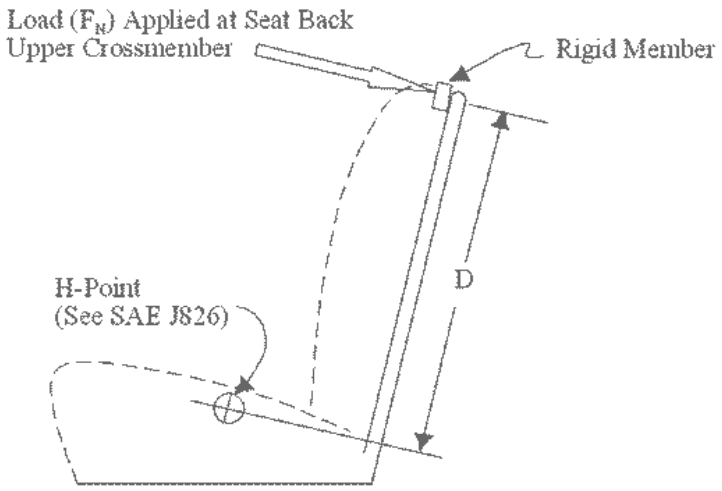

Figure 1-1 Force on the top cross member of the backrest creating a moment of 373 N-m about H-point in accordance with FMVSS 207 [5].

David C. Vaino at General Motors Corporation in 2003 developed a proposed quasi static test in order to analyze the performance of high retention seats during an event of rear impact [6]. The quasi static test was simulated by placing a hybrid dummy in the seating position and then displacing the hybrid dummy rearward into the seat with the help of a hydraulic ram. The quasi static test was aimed at accessing the strength deflection characteristics of the seat and the interaction of the occupant with the seat in an event of rear impact [6]. The load is transferred to the seat by a distributed force through the upper torso and buttocks of the hybrid dummy. The strength deflection characteristics were obtained by calculating the moment developed about the H-point and deflection of the seat from the force and displacement data of the hydraulic ram. Twenty different seats were studied using the quasi static test developed in order to assess their performance [6].

In a study conducted at Dura Automotive systems, the FEA predictions for an automotive front seat subjected to luggage retention test in accordance with ECE R17.07 [7] are correlated with physical test results. The test was conducted on a simple prototype seat model in order to

evaluate the damage caused by rear luggage impact on seat structure. The sled test is simulated by impacting the seat from the rear with a rigid luggage block. The design, simulation and testing is done on a full scale automotive seat by integrating individual components [7]. The structural components of the seat are modeled using shell elements. The bolt connection between different parts in the finite element model of the seat is represented by using rigid multi point constraints for the bolt heads on the two parts connected by beam elements. Contact is defined between different components of the seat and between the rigid luggage block and the seat model. An elastic-plastic material model for ductile steel with a yield strength of 600 MPa at 0.01 nominal strain, ultimate tensile strength 680 MPa at 0.1 nominal strain, and failure strength of 500 MPa at 0.8 nominal strain is used to represent the material used for seat structural components [7]. The sled test is simulated using LS-Dyna explicit solver. A prototype of the seat is built and physical testing is carried out in order to correlate the results. Comparison of finite element simulation data with the test data shows a reasonable correlation establishing confidence in finite element modeling techniques [7].

The ECE R17 regulation applies to the strength of seats and their anchorages for production seats in the European Union. The regulation sets standards for strength of the seat-back and its adjustment systems. The strength of a seat is important to protect the occupant from severe crash loads in an event of rear impact. The occupant is pushed back against the backrest causing the backrest to bend about the base frame. Because of the severe load of the occupant against the backrest, rear impact load is the primary driver for the backrest structural design. Rear impact loads also apply large forces to the base frame and height adjustment legs and slider rails.

In accordance with ECE-R17 [3], the moment test setup for rear impact specifies a force directed towards the rear applied to a body form which simulates the SAE J826 manikin back and contacts the backrest. In a study conducted by Hesser and Thompson [8,9], the ECE R17 moment test simulated on a finite element model of an reference seat by applying a force directed towards

the rear on the top cross member of the backrest creating a moment of 530N-m about the H-point in accordance with ECE R17, see Figure 1-2. Static analysis with a linear elastic material for the stamped sheet metal backrest frame was considered in order to simulate the quasi static moment test [8,9]. The analysis is used to predict the stress in the seat frame prior to yield. For this simplified analysis, the backrest was isolated from the base frame and restrained at the bearing surfaces of the base frame connectors and the load path between the SAE J826 body form and backrest was approximated by applying a force on the top horizontal member. The results from this analysis showed that for a moment loading of 530 N-m and simplified boundary conditions, the maximum stress exceeded the yield stress of 305 MPa for low carbon 1010 steel by 30% and occurred in a tapered section of the side vertical frame members of the backrest. To better represent contact interaction between the body form and backrest, a distributed load along the upper part of the vertical frame members was also applied. The results from this load path reduced the maximum stress to 300 MPa at the tapered section of the vertical members. This study shows that the analysis results are highly dependent on the accurate representation of the body form contact interaction with the backrest. A similar linear static analysis of a die-cast magnesium alloy backrest frame was carried out by Grujicic and Hodges in [19]. Accurate finite element modeling of an reference seat which has passed ECE R17 moment test requirements is important to provide a benchmark reference to compare new concepts and designs which reduce weight while maintaining minimum test requirements.

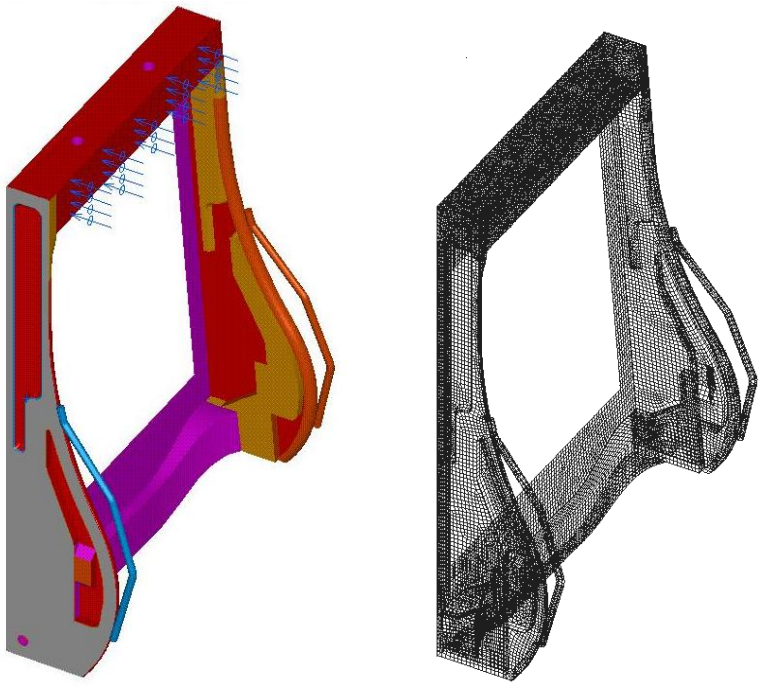

Figure 1-2: Geometric and Finite Element Model of Reference Backrest with load applied on the top cross member simulate ECE R17 moment test, from [8,9].

1.2 Thesis Objective and Outline

The objective of the work is to accurately simulate the moment test on the reference automotive front seat in accordance with ECE R17. The reference seat considered has passed the physical test. The accurate load path representation by surface contact interaction between the SAE J826 body form and the backrest is important in order to closely match the simulated moment test to the physical test. In order to achieve the objectives, the moment test is simulated by including a rigid body model of the SAE J826 body form in the test setup. The finite element simulation of the reference seat is conducted beyond the component level by using a complete seat model formed by integrating the major structural components of the backrest, connector, base frame, and slider rails. Contact within the seat structure is defined in order to simulate joints between side flanges and cross tube members of the base frame. Contact modeling is also used to

simulate the interaction of the body form with different components of the seat. Height adjustment, front tilt adjustment and the backrest tilt angle adjustment locking mechanisms are represented in the finite element model using rigid connections. The bolt connections between different parts in the model are represented using multi-point constraints. An elastic-plastic material model is used to model the structural components of the seat. Different grades of steel with low, medium, and high strength are considered for the different components. In order to confirm the strength requirements, moment deflection characteristics of the seat are studied in accordance with ECE R17. The moment test is simulated using two complementary loading cases, constant horizontal force and constant angular velocity on the reference seat with in order to evaluate the performance of the seat. Since the ECE R17 regulations do not provide precise specifications for the height of the applied force and test setup for the body form pivot mechanism, a study is conducted in order to understand the influence of body form rotation and height of the body form above the H-point. The influence of plastic material properties of different grades of steel used for the seat model, front mesh contour on the backrest and connection between the backrest and connector are modified to analyze the influence of load path on moment deflection characteristics of a seat.

An outline of this work is as follows:

Chapter 2 explains the function and working of different components of the reference seat used in this study obtained by reverse engineering of the physical seat. Major load carrying structural components of the seat including the base frame, backrest, slider rails, and connectors are described. Seat adjustment features and locking mechanisms are also described.

Chapter 3 describes the procedures of testing the strength of a seat in an event of rear impact in accordance with ECE R17. The procedure for locating the H-point of a seat is followed by two different simulation methods of testing the seat for strength and deflection characteristics.

Chapter 4 describes the elastic-plastic material model used for the load carrying structural components of the seat. The different grades of steel used are described and the procedure for converting nominal stress and strain to true stress and strain, required for input to ABAQUS/Explicit is explained.

Chapter 5 describes the geometrical CAD model and associated finite element model for the seat. The contact interactions between different components of the seat, rigid connections, and multi-point constraints for modeling the locking mechanisms and bolted joints are explained.

In Chapter 6 the moment test is simulated in accordance with ECE R17 using the developed nonlinear finite element model. The effects of changing different parameters on the moment deflection characteristics are discussed.

Error! Reference source not found. provides the conclusions and suggestions for future work.

CHAPTER 2

DESCRIPTION OF A REFERENCE AUTOMOTIVE FRONT SEAT

Automotive seats provide comfort, ergonomics and safety to the occupant while traveling. The primary function of a seat is to provide seating space for the passengers and support them in the event of accidents. Most automotive seats are designed in a similar fashion with an adjustable seating space and back support providing ideal ergonomic driving conditions. Seats essentially consist of a skeletal structural frame work designed to carry load. Body contact areas are covered with PUR foam. The structural framework provides shape and strength to the seat while PUR foam provides comfort and ergonomic driving conditions. The structural components of the reference seat studied in this work are shown in Figure 2-2. The seat has four manual adjustment features for comfort and safety (a) Backrest angle adjustment, (b) Height adjustment, (c) Longitudinal adjustment, and (d) Front tilt adjustment. Movements of different adjustment features in the seat are restrained by locking mechanisms mounted on the side flanges of the base frame.

2.1 General Description of a Reference Front Seat

The seat nomenclature typically consists of (a) Backrest, (b) Head-rest, (c) Seat pan, (d) Base frame, and (e) Slider rails. The backrest of the reference seat is made of stamped low carbon steel components consisting of two vertical members with cross members attaching at the top and bottom as shown in Figure 2-3. The backrest has an open region which PUR foam is contoured and supported by springs connecting the back rest vertical members. Connectors located on both sides are mounted in slots on the backrest and connected to an inner cross tube which is locked on one side with a backrest angle adjustment gear on the base frame. The adjustable head restraint is a U shaped circular tube covered with PUR foam and is attached to the top cross member of the backrest. The base frame consists of side flanges with cross tubes at the front and back as shown

in Figure 2-4. The connectors pivot on the side flanges and mesh with a gear on a tube located inside the back tube. The inner tube meshing with the connector is locked to the side flange by a larger gear on the inner tube on one side only. The seat pan provides seating space and consists of two parts, one mounted in the front and other in the rear of the side members of base frame as shown in Figure 2-5. The front and rear parts of the seat pan are connected by springs creating a cavity in the base frame filled with PUR foam for comfort as shown in Figure 2-5. The seat has a thigh support pad for comfort which can slide out from the seat pan. The base frame is supported by four legs at four corners of the seat. The legs are welded to the ends of the cross tubes and are pinned at the slider rails. The legs are connected to the tubes and pinned to the slider rails for height adjustment. The slider rails are bolted to the floor of an automobile at four locations, two on each side. The slider rails are used to adjust longitudinal position of the seat. The overall reference seat dimensions are shown in Figure 2.1.

Figure 2-1: Overall Dimensions of the Reference Seat

Figure 2-2: Reference Seat Nomenclature

2.1.1 Backrest and Backrest Base Frame Connector

The role of a backrest is to provide comfort to the occupant and support the occupant in an event of severe impact to the automobile. A significant amount of load acts on backrest of the seat during the event of rear impact of the vehicle as the occupant is pushed rearward. Thus, the backrest has to be designed for structural rigidity and strength to a load acting rearward. The reference backrest is essentially a rectangular boxed structure made from low-carbon stamped sheet metal with vertical members connected by cross members at the top and bottom as shown in Figure 2-3. The functions of the vertical members are to support the backrest in bending. Vertical members are tapered and run from bottom to top of the 580mm long backrest on either side. They are made from stamped low carbon steel sheet metal formed in the shape of a C-Section. The

tapered vertical members have 130mm depth at the bottom and 55mm depth at the top. A circular rod of 8 mm diameter is welded to the lower portion of the vertical member for additional side bolster of an occupant. The two vertical members are separated by a distance of 450 mm and connected by cross members at the top and bottom of the back rest forming a rectangular open boxed structure. The vertical members are 1 mm thick stamped flanges with C-lips at front and back. The vertical flanges are designed with stamping features to improve its stiffness in bending. The top cross member has a 1 mm thick rectangular cross section welded to the vertical members at the top. The top cross member has two holes fitted with bushings to mount the U-shaped head restraint. The bottom cross member is a 1 mm thick C-section welded to the vertical members at the bottom.

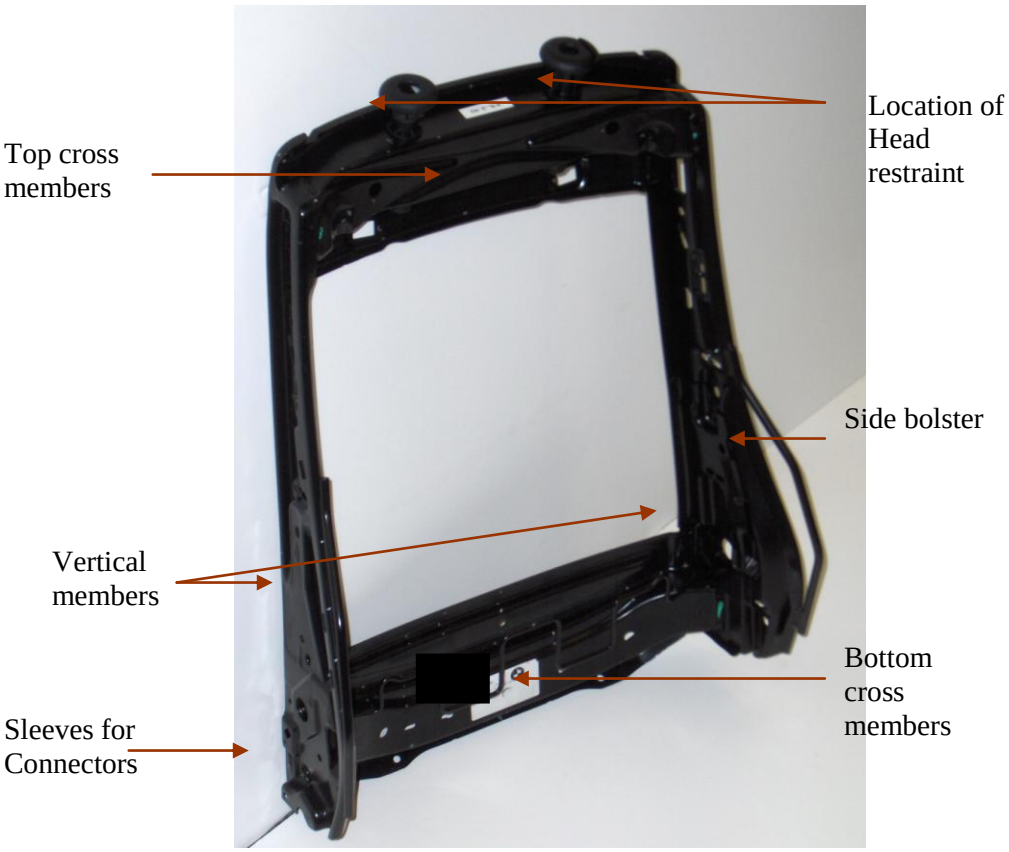

Figure 2-3: Reference Backrest Nomenclature

The backrest is connected to the base frame by a hardened steel plate connector with bearing surfaces on one end and gear teeth riveted to the other end. The connectors are located in a sleeve pocket formed by attaching a support structure constructed of sheet metal welded to the lower flange region of the vertical members of the backrest. The connectors are inserted into sleeves in the backrest and are bolted on the side of the vertical members and pivot about a pin on the side flanges of the base frame. During loading, the connector plate bears against the slot in the backrest sleeve at the top end and meshes with gears on the inner cross tube at the rear of the base frame. A locking gear welded on one side of the tube inside the rear cross tube is locked on one side and alloys backrest angle adjustment.

The backrest is made of stamped components of low carbon steel welded together at discrete locations. Short continuous welds are used strategically at different locations to connect the backrest structural components to define the load path and maximize the strength of the backrest structure. The 1 mm thick support structure welded at discrete locations to the back rest not only supports the connector but also adds stiffness to the vertical members in bending. The rectangular shape of the backrest creates an open region at the center which is spanned by PUR foam supported by springs connecting the vertical members at different locations on the back rest.

2.1.3 Base Frame

The function of the base frame is to provide structural rigidity to seat and act as a support platform to mount the backrest. The base frame supports load on the backrest during rear end collision and load from the seat belt on the door side of the base frame during frontal impact of an automobile. The base frame is an open box frame with two side flanges connected by cross tube members at the front and rear as shown in Figure 2-4. The frontal impact causes substantial bending load to act on the side flanges on door side from lap belt pull-off and the rear impact also induces bending load on side members through the connector pin and the back rest tilt locking mechanism on the side flanges. The side flanges generally have C-section shapes and separated by a distance of 420 mm designed to primarily resist bending load. The side flanges are free to rotate about the front and rear cross tubes. The 2 mm thick stamped side flanges provides mounting locations for the different mechanisms. The backrest tilt locking mechanism, height adjustment locking mechanism, front tilt locking mechanism and seat belt are mounted on the side member located on the door side. The connector pivots about a pin on the side members and locked to the door side member by a meshing lock gear as shown in Figure 2-4. Mounting locations are provided at the front and rear of side members to position the two piece seat pan.

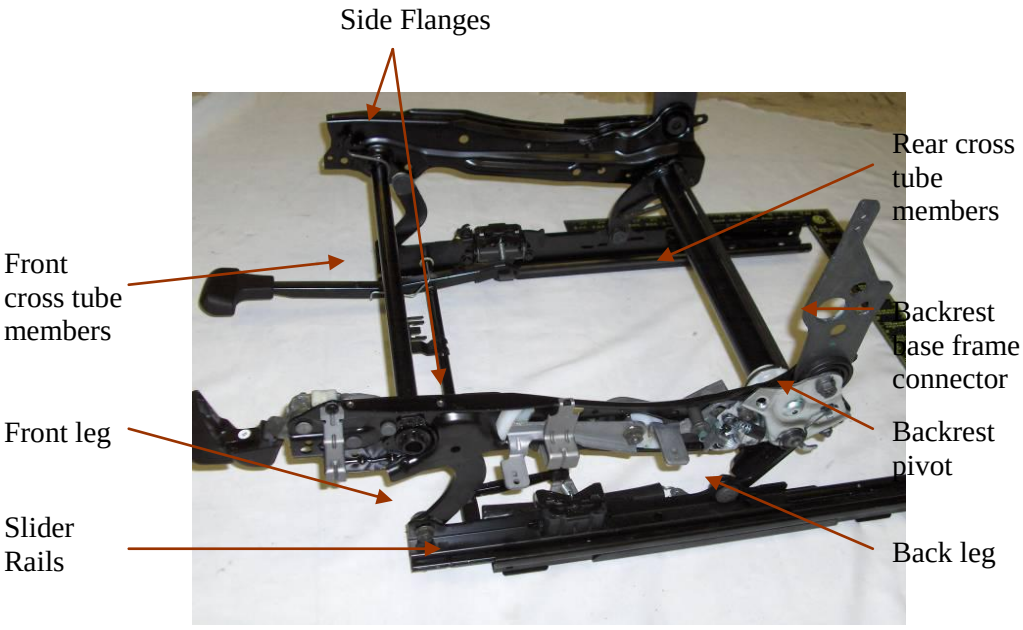

Figure 2-4: Reference Base Frame Nomenclature

The side members are made of stamped low carbon steel. The 2 mm thick front cross tube member 18 mm in diameter and 1.75 mm thick rear cross tube member 30 mm in diameter, connect the two side members separated by a distance of 420 mm. The open box structure of the base frame provides clearance for positioning mechanisms on the side members as shown in Figure 2-4 and is designed to withstand severe offset, front, rear, and lateral loads. The base frame is a major weight contributor to the seat as it has to be strong to withstand the severe loading conditions. The legs on the in-board side are bent slightly causing the base frame to offset from the mounting locations on the slider rails to accommodate the transmission tunnel passing under the seat.

2.1.4 Seat Pan

The seat pan consists of two pieces, one mounted in the front and the other mounted on the back as shown in Figure 2-5. The seat pan is mounted on the front part of the side flanges of the base frame and a rear frame mounted on the rear part of the side flanges. The front portion of the seat pan supports body forces and also provides side bolster for the occupant. The two pieces of the seat pan are connected by springs. The springs not only support the PUR foam but also provide compliance to the seating area. A thigh support pad provided for comfort slides out from the seat pan and can be locked and adjusted.

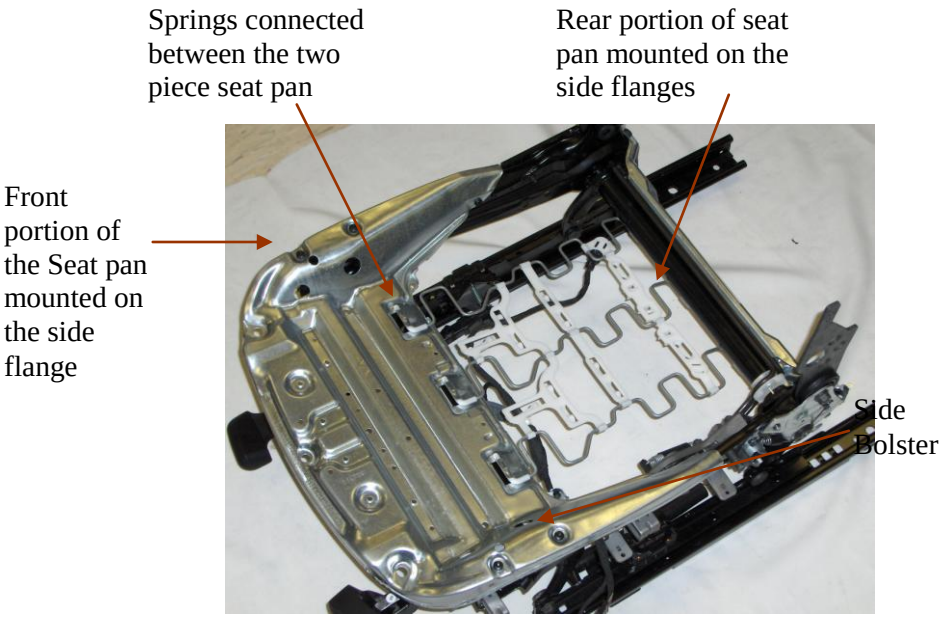

Figure 2-5: Reference Seat Pan Nomenclature

2.1.5 Slider Rails

The primary function of the slider rail is to attach the base frame along with backrest to the floor of vehicle as shown in Figure 2-2. The two slider rails are secured to the vehicle floor by bolt connections at 4 mounting locations. The slider rails are 450 mm long are separated by a

distance of 420 mm. Slider rails are 3 mm thick in order to transfer the severe loads acting on the base frame and backrest to the vehicle floor. In addition, on the in-board side, large pullout loads from the seat-belt bracket are resisted. To allow adjustability, the slider rail has two parts connected by rollers which can slide one over the other as shown in Figure 2-6. The relative sliding between the slider rail components moves the entire seat in the longitudinal direction. Relative sliding of the two slider rail components is locked by four cylindrical pins engaging them together. A lever is used to activate and deactivate the lock in order to adjust the seat position through a range of 250 mm in the longitudinal direction with respect to the floor. The slider rails are made of low carbon steel. The strength requirement of the slider rails makes it a major weight contributor of the seat.

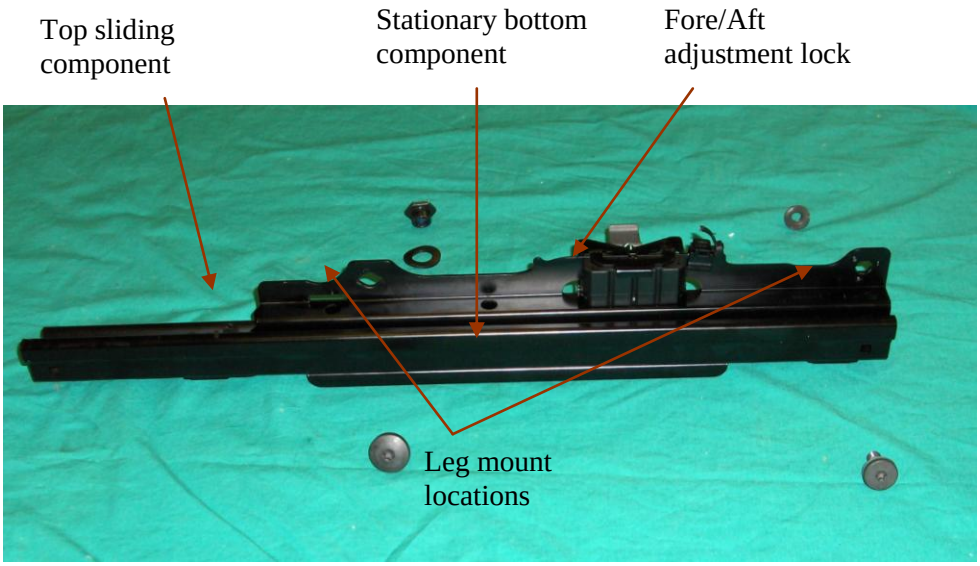

Figure 2-6: Reference Slider Rail

2.1.6 Backrest Angle Adjustment

The back rest angle adjustment mechanism allows the backrest to change and lock angle with respect to the base frame. The mechanism consists of a backrest base frame connector, inner tube with gears and a locking gear supported by cams as shown in Figure 2-7. The back rest angle can be adjusted through a range of 55 degrees in 7 steps by activating the backrest angle adjustment mechanism lever. The backrest base frame connectors pivot about a point on the side members on either side of the base frame side flanges and meshes with gears on an inner tube passing through the rear cross tube member as shown in the Figure 2-4. The meshing teeth between the connector and inner tube are 12 mm thick. The 4 mm connector is made of stamped high strength steel in order to transfer the load from the back rest to the base frame. The backrest angle adjustment is restrained by locking the large gear on the inner tube. The backrest is locked on only one side of the base frame. Thus, the locking gear, cams and lever are mounted on the left side member of the base frame. Two torsion springs, one on each connector prevents the backrest from collapsing while adjusting it in an unlocked position. The locking gear is 4 mm thick which is determined by the locking forces required to withstand a severe load acts on the back rest in rear impact. The backrest tilt can be adjusted by activating the mechanism. The mechanism is activated by pulling the lever up. The cam disengages the lock gear meshing with the large gear. The inner tube is free to rotate and a force applied to the backrest by an occupant back will rotate it about a pivot point on the side member through a required angle. The lever is released to deactivate the mechanism thus locking the backrest.

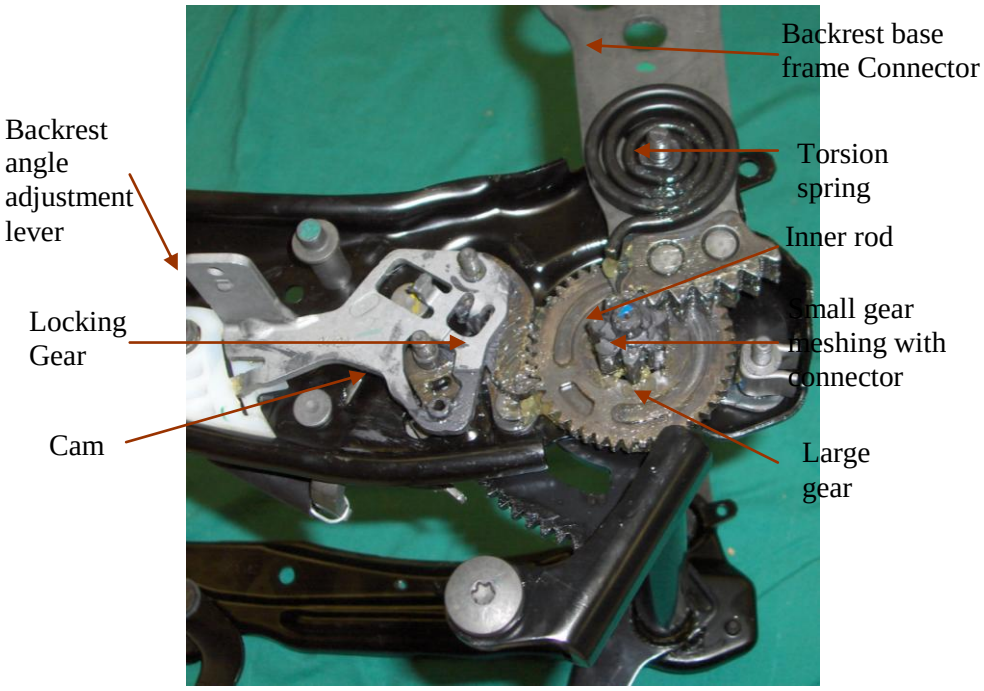

Figure 2-7: Backrest Angle Adjustment

2.1.7 Height Adjustment Mechanism

The height adjustment mechanism adjusts the height of the seat with respect to the slider rails. The height adjustment mechanism consists of a height gear which is an integral part of the back leg and locking gear supported by a cam as shown in Figure 2-8. The range of motion of height adjustment is 55 mm in the vertical direction and 35 mm in the longitudinal direction which is adjusted in 13 steps. The height adjustment is locked at only one leg of the seat. The locking gear and cams are mounted on the inner side of left side member as seen in Figure 2-8. The height gear is 5 mm thick and meshes with a locking gear mounted on the side member. The height gear is made of stamped low carbon steel. The locking gears and cams are made of stamped high carbon steel. The height gear is a part of the back leg and is welded to the back tube. A torsion bar is attached across the back legs to prevent the seat from collapsing while adjusting the height. The height gear prevents the seat from collapsing by withstanding the loads

during front and rear impact of an automobile. The back legs are 90 mm long and are welded to the rear cross tube member at one end and pinned to the slider rails on other end. The back leg on the left of occupant has an integrated height adjustment gear locked by a height adjustment mechanism on to the side member. Under severe loading conditions the leg has a flat region which stops on slider rail to support the seat under severe deformation in the lowest position. The front legs are 90 mm long with one end pinned to the front tilt gear welded to the front tube and the other end pinned to slider rail. The front and back legs are 5 mm thick. The height adjustment mechanism is activated by pulling the lever up. The cam rotates and disengages the locking gear from the height gear. The downward force on the seat by a person is used to adjust the height of the seat. The height of the seat is altered because of the front and rear cross members along with legs rotate about a stationary point on the slider rail. The relative rotation of the side members with respect to front and rear cross members align the seat horizontal to the floor at all positions. The lever when released deactivates the mechanism locking the height adjustment of the seat.

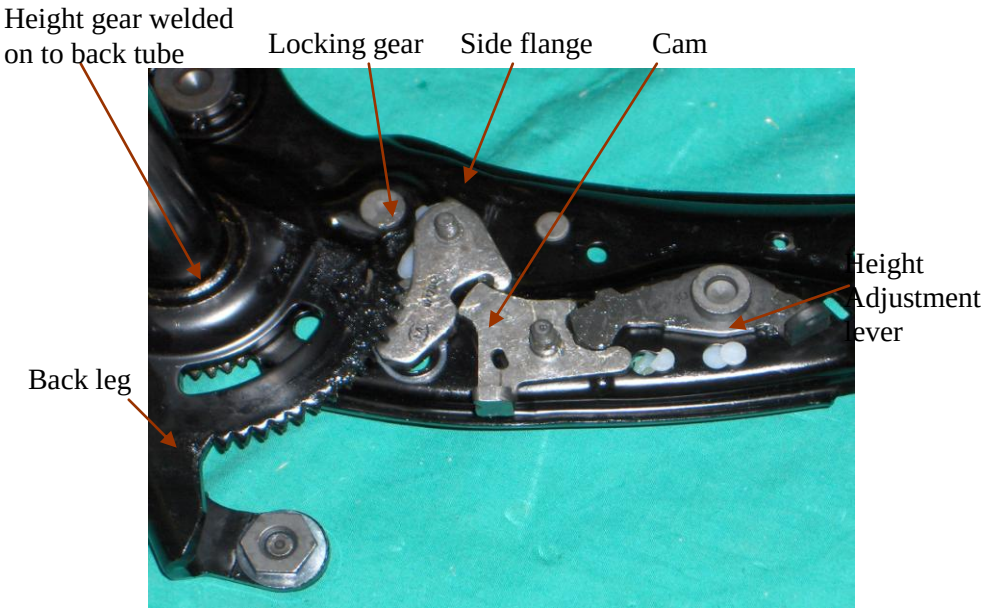

Figure 2-8: Height Adjustment Mechanism

2.1.8 Front Tilt Adjustment Mechanism

The front tilt mechanism primary function is to adjust the front tilt angle of the seat. The front tilt mechanism consists of a tilt gear welded to the front cross tube member and locking gear supported by a cam as shown in Figure 2-7. The range of motion of the front tilt is 5.7 degrees which is adjusted in 7 steps. The front tilt is locked on the left side member of the base frame. The locking gear and the cam are mounted on the inner side of side members as seen in Figure 2-7. The 5 mm thick tilt gear is welded on to the front cross tube member and attached to front leg by a bolt connection. The tilt gear is made of stamped low carbon steel. The locking gear and cams are made of stamped high carbon steel. The front tilt adjustment mechanism is activated by pulling the lever up. The cam rotates and disengages the locking gear from the tilt gear. The force applied at front of the seat by an occupant will adjust the tilt location. The tilt gears along with the front cross member rotate about the front leg changing the angle of the seat. The lever when released deactivates the mechanism locking the front tilt adjustment of the seat.

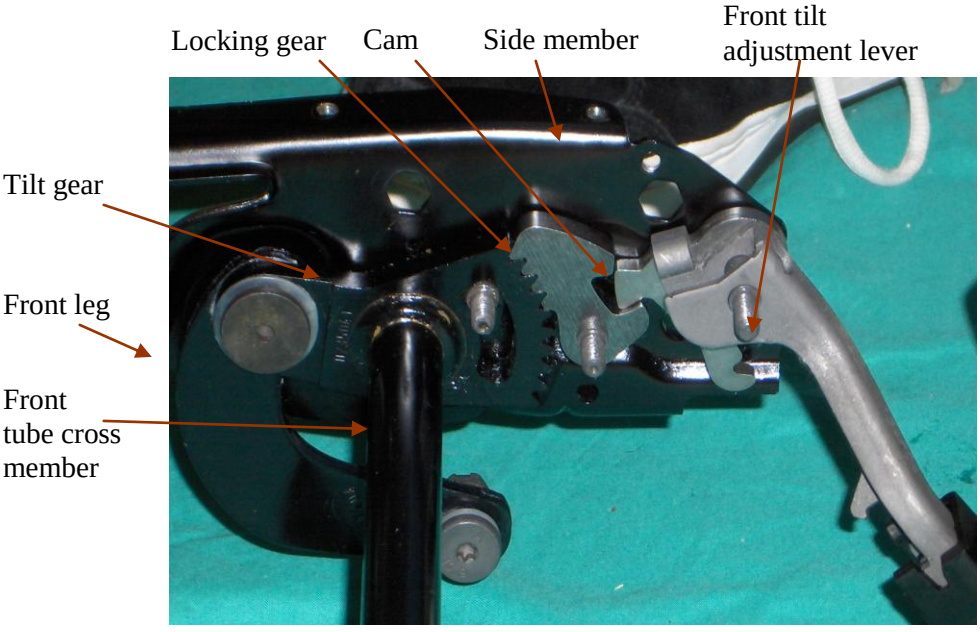

Figure 2-9 Front Tilt Adjustment Mechanism

CHAPTER 3

SIMULATION OF TEST REQUIREMENTS FOR AUTOMOTIVE FRONT SEAT

Automotive seats are physically tested for strength, deflection, and energy absorption in an event of vehicle rear end, front end, and side impact loads mandated by government agencies prior to approving the seat design for active duty. Automotive vehicles driven in the European Union must satisfy the requirements of ECE R17 [3] regarding seats. The structural design of a complete seat is primarily driven by the strength requirement in an event of vehicle crashes. The seat has to support the weight of a person and also resist severe static and dynamic loading during an event of accident. During rear, frontal and side impacts of automobile, structural members are the load bearing components in a seat. The moment requirements of typical reference seats for rear impact of an automobile are often several times higher than the European Union standard ECE- R17. In Chapter 4, the strength of the seat in rear impact is measured by the moment resisted by a rear ward load acting on the backrest from a body form represented contact with the occupant. The moment-deflection characteristic of the reference seat in an event of rear impact is simulated by a quasi-static finite element analysis using ABAQUS/Explicit.

3.1 Moment Test for Rear Impact

In order to properly load the seat during simulation of rear impact, the H-point location representing the physical pivot of the occupant hip area and initial torso angle has to be measured. A three dimensional H-point machine represented by SAE J826 as shown in Figure 3-1 is used to measure the initial torso angle and H-point location. The three dimensional H-point machine represents a person sitting in a seat. The manikin consists of a back plate representing the torso and a pelvis plate representing the thighs connected mechanically by a hinge joint at the H-point. The thigh bar is a reference base line attached to the pelvis plate and is connected to the lower leg segments by a T-bar. The foot assemblies are attached to the lower legs segments. Torso weight

hangers represent the weight of the torso and rest on the back plate. The back plate angle is measured by the inclination of height probe attached to the manikin at the H-point with respect to the vertical. Weights are attached to the manikin at different hanger locations to represent the weight of a 75 kilogram male person [3].

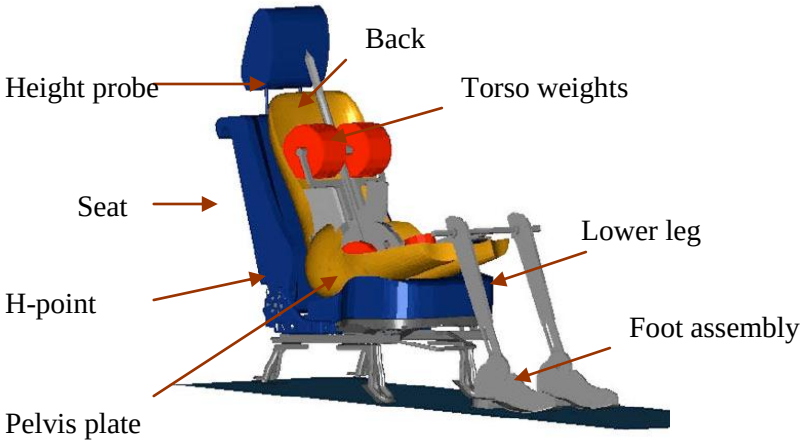

Figure 3-1: Illustration of Three dimensional H-point Manikin [10]

The seat is placed on a test rig and rigidly restrained. The seat is adjusted to normal driving position and the H-point manikin is placed in such a way that the center plane of the occupant coincides with the center plane of the H-point manikin model. The legs are positioned on the floor to match normal driving position of the occupant. The manikin is pushed rearward into the seat by applying a force of 100N directed towards the rear at the location of H-point. The weights are positioned at hanger locations on the manikin. The H-point location is measured with respect to the vehicle reference system. The height probe is placed in a fully rearward position and the initial torso angle is measured with respect to normal at the back angle quadrant. The location of the H-point and initial torso angle required to apply a quasi-static load in rear impact are measured [3].

ECE - R17 regulation applies to the strength of seats and their anchorages, to the design of rear parts of seat backs, to the characteristics of head restraints, and to devices intended to protect the occupant from the danger resulting from the displacement of luggage in a frontal impact of vehicles. The regulation sets standards for strength of the seat-back and its adjustment systems, test of strength of the seat anchorage and the adjustment, locking and displacement systems, performance of the head restraint, energy dissipation on the seat back, and head restraint. The strength of a seat is important to protect the occupant from severe crash loads in an event of rear impact. The occupant is pushed back against the backrest causing the backrest to bend about the base frame. Because of the severe load of the occupant against the backrest, rear impact load is the primary driver for the backrest structural design. Rear impact loads also apply large forces to the base frame, height adjustment legs, and slider rails.

The moment test setup for rear impact simulation is performed in accordance with ECE-R17 [3]. A force directed towards the rear is applied to a body form which simulates the SAE J826 manikin back and contacts the backrest. The magnitude of force is measured based on the resulting moment about the H-point SAE J826 manikin as shown in Figure 3-2. The seat must satisfy the requirements in all positions of the longitudinal and height adjustment features and also in all positions of the angle adjustment feature.

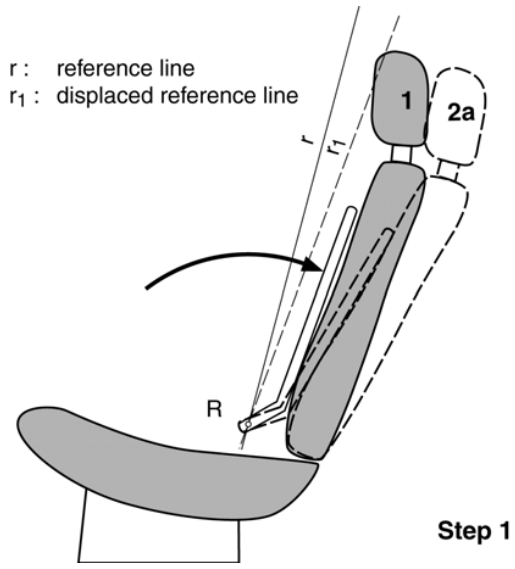

Figure 3-2: ECE R17 Test Setup for Backrest Moment Load [3]

The test procedure requires a force directed toward the rear. Up to an intermediate torso angle, the seat must withstand a moment denoted M_0 with units N-m. The magnitude of M_0 is several times larger than the ECE-R17 requirement. At the end of deformation travel, a minimum moment of $0.56\,M_0$ N-m must be maintained. Along the deformation path, the moment must not fall below a value of $0.56\,M_0$ N-m. Over the entire deformation fracturing or cracking must not occur on any part pertinent to strength. The locking mechanisms and adjusting devices must remain in the set positions. The seat should deform in a controlled manner throughout the travel angle. The test is conducted on a machine in accordance with ECE R17 as shown in Figure 3-3. The seat is restrained on a rigid floor and an upright SAE J826 manikin body form is pivoted about the H-point of the seat. The hydraulic ram pushes the body form against the seat and the moment of the seat is measured at the H-point.

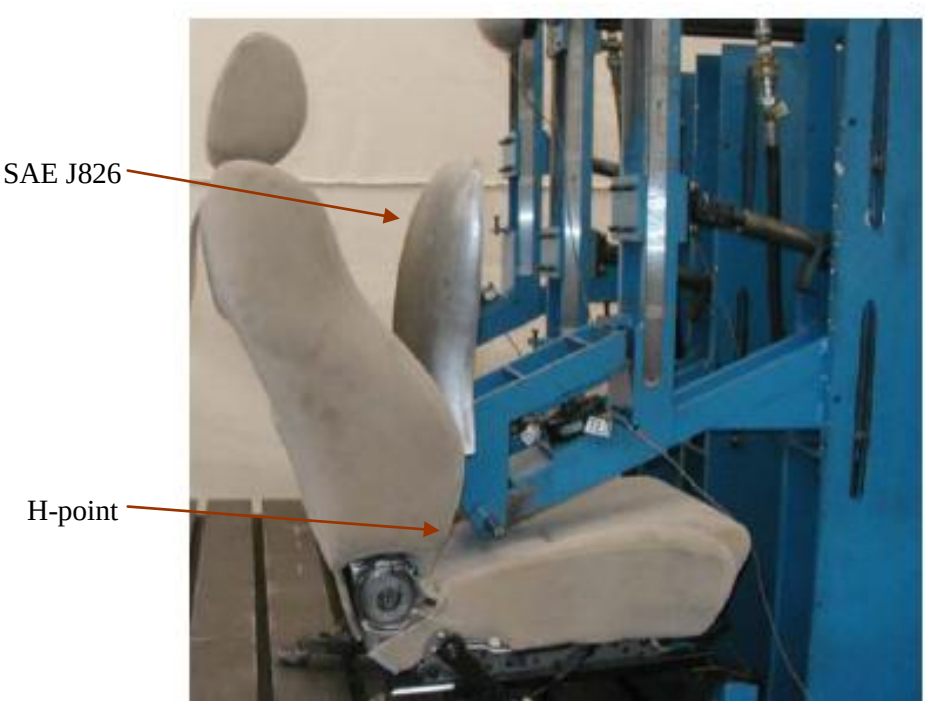

Figure 3-3: Test Setup for ECE R17 Backrest Moment Test [11]

3.2 Finite Element Simulation of ECE R17

The finite element simulation of the strength requirement of a seat in rear crash test is carried out in accordance with ECE R17. The finite element analysis is performed using two simulations; constant horizontal force and constant angular velocity of the body form to analyze the strength of a seat in rear impact. SAE J826 manikin body form representing occupants back is modeled in ABAQUS as a rigid body as shown in Figure 3-4. Splines in ABAQUS have been used to model the body form to represent the SAE J826 manikin body form (A physical SAE J826 manikin was not available). The ABAQUS body form is 340 mm wide and 515 mm long. A mass of 10 kg and mass moments of inertia with respect to a reference point of the rigid body form are Ix = 884083.33 kg-mm^2, Iy = 96333.33 kg-mm^2, and Iz = 999683.33kg-mm^2.

Figure 3-4 (Left) SAE J826 Manikin Body Form [12] (Right) ABAQUS Body Form Model

3.2.1 Moment Test (Constant Horizontal Force)

In the first simulation model of the moment test, a horizontal force is applied on the body form which then makes contact with the backrest model. The moment is measured from the changing perpendicular distance during deformation and the torso angle measured from the rotation of the H-point. In the ABAQUS model, the rigid body form is connected to a rigid link at the reference point. The body form along with the link rotate about the pivot point placed at the H-point at the bottom of the rigid link. The body form is located in front of the seat in such a way that the pivot point of the body form coincides with the H-point of the seat. A force F is applied at the reference point in the horizontal direction creating a moment of $M_1 = Fd_1$ about the H-point of the seat at initial position measured by d_1 as shown in Figure 3-5. The force $F = M_{1/}d_1$ is kept horizontal and constant throughout the deformation of the seat. The moment created by the force F about the H-point through the deformation of the seat is calculated from the changing perpendicular distance between the line of action of the force and H-point using

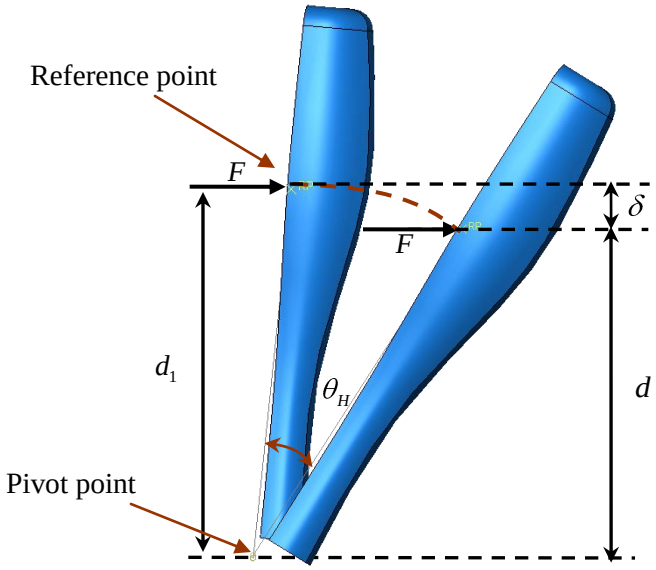

Figure 3-5: Moment Load from Constant Horizontal Force F Simulating ECE-R17 Test Load

$$M = Fd = M_1(\frac{d}{d_1}) \qquad \textbf{(3-1)}$$

In the above, F is the applied force, $d = d_1 + \delta$ is the vertical distance above H-point, d_1 is the initial vertical distance above H-point, and δ is the negative displacement of the reference point.

The moment deflection characteristics of the seat are calculated by measuring the rotation of the body form at the H-point and the vertical displacement of the point at which the force is applied. In ABAQUS, the vertical displacement is time dependent and is given by $d(t) = d_1 + \delta(t)$. The H-point rotation angle as a function of time $\theta_H(t)$ is inverted to give time as a function of angle $t = f(\theta_H)$. The moment is calculated from the measured vertical displacement and input force from $M(t) = F(t)d(t)$. Using $t = f(\theta_H)$ the moment can also be expressed in terms of angular displacement as $M(\theta) = F(\theta)d(\theta)$.

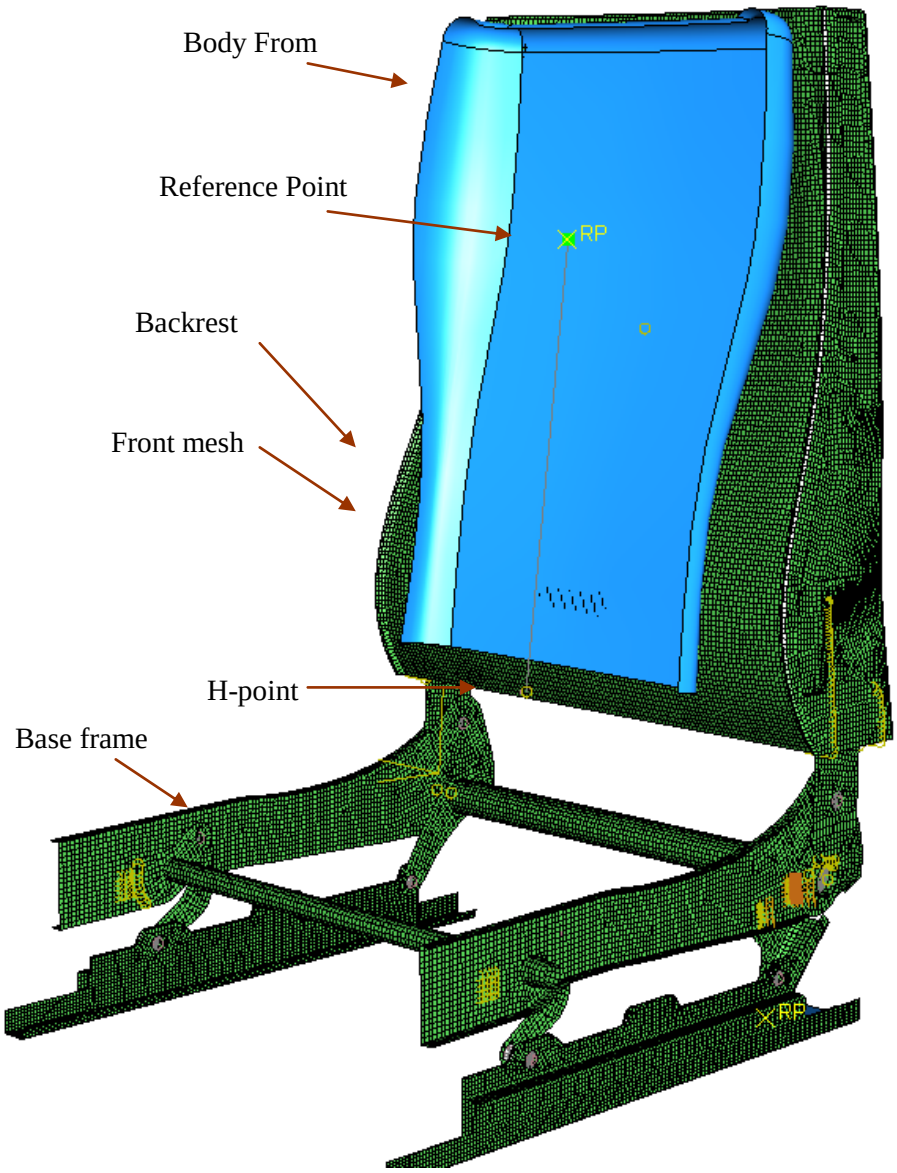

Figure 3-6: Finite Element Setup for Rear Impact Moment Test (Constant Horizontal force)

Further details of the ABAQUS model of the loading follow. The body form is placed in front of the seat. The reference point of the body form is connected to the H-point by a rigid link. The body form with the rigid link is free to rotate about the H-point axis. The rigid link connects all degrees of freedom between the H-point and the body-form reference point except rotation

about the H-point. As a result, the body form is free to rotate independently about reference point axis. The relative free rotation between the H-point axis and the reference point axis helps the body form maintain contact uniformly over the entire front area of the backrest. ABAQUS finite element simulations showed that if the rotations of the body form about the H point axis are constrained to the reference point, the body form contacts only on the upper portion of the backrest.

The body-form and backrest are initially positioned at a nominal 25 degrees torso angle. In order to create a maximum moment of M_0 N-m after an intermediate angle has been reached, a constant force is applied on the body form at the reference point in the horizontal direction. The force is ramped up to the maximum value in 10 sec using a smooth step function and is maintained constant for the rest of the analysis. In ABAQUS, the smooth step forcing function is defined by a fifth order spline function given by

$$F(t) = \begin{Bmatrix} F_0(10 - 15\xi + 6\xi^2)\xi^3, & 0 \le t \le 10\,\text{sec} \\ F_0 \quad , & 10 \le t \le 40\,\text{sec} \end{Bmatrix} \qquad (3\text{-}2)$$

where $\xi = t/10$ sec, F_0 is the maximum input force, and t is time in seconds.

The length of the pivot arm connecting the H-point and the reference point is 360 mm above the H-point. The input moment $M_1 = Fd_1 = 1.12\,M_0$ N-m at the reference point of the seat at the initial torso angle of 25 degrees and represented by the forcing function (3-2) is shown in the Figure 3-7.

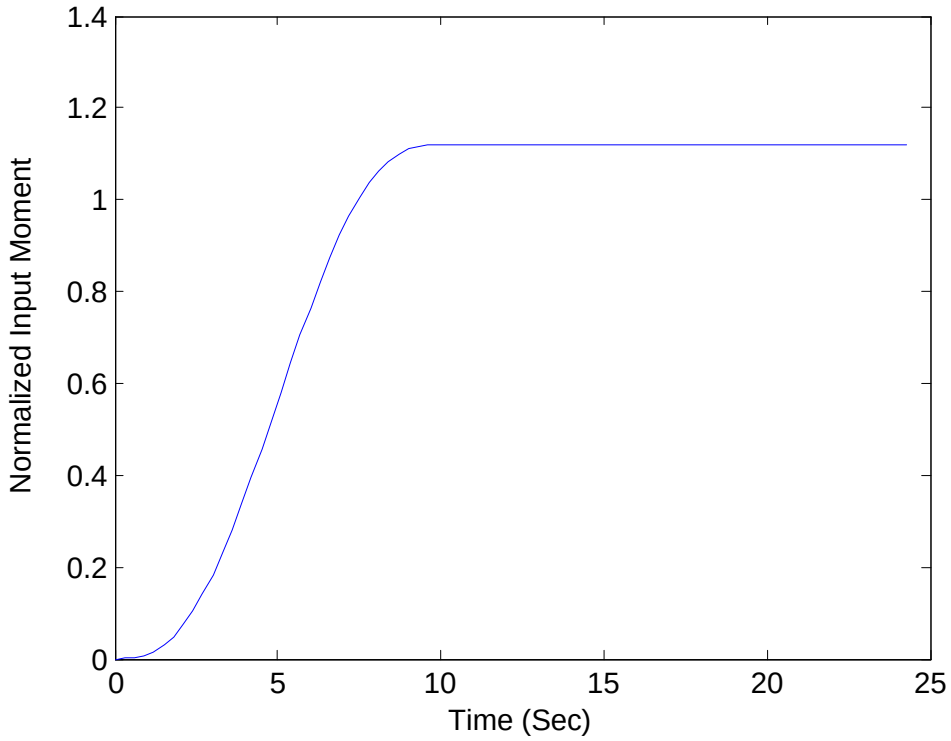

Figure 3-7: Smooth Step Amplitude Function for Input Moment, $M_1 = Fd$.

3.2.2 Moment Test (Constant Angular Velocity)

In this simulation, instead of applying a constant force, the body form is rotated about the H-point axis with a constant angular velocity and the moment reaction at the H-point assumed at the bottom of the body form is computed. The moment reaction is measured starting from 25 degrees up to 50 degrees torso angle. The body form is positioned in accordance to ECE R17 as shown in Figure 3-2. The body form is positioned in front of the seat in such a way that the reference point of the body form coincides with H-point of the seat located at a height of 70 mm from the seating surface and 25 mm in front of the backrest. The reference point is located at the bottom edge of the body form which aligns with the H-point axis. In finite element analysis a

moment is developed on the seat by displacing the body form against the backrest as shown in Figure 3-8.

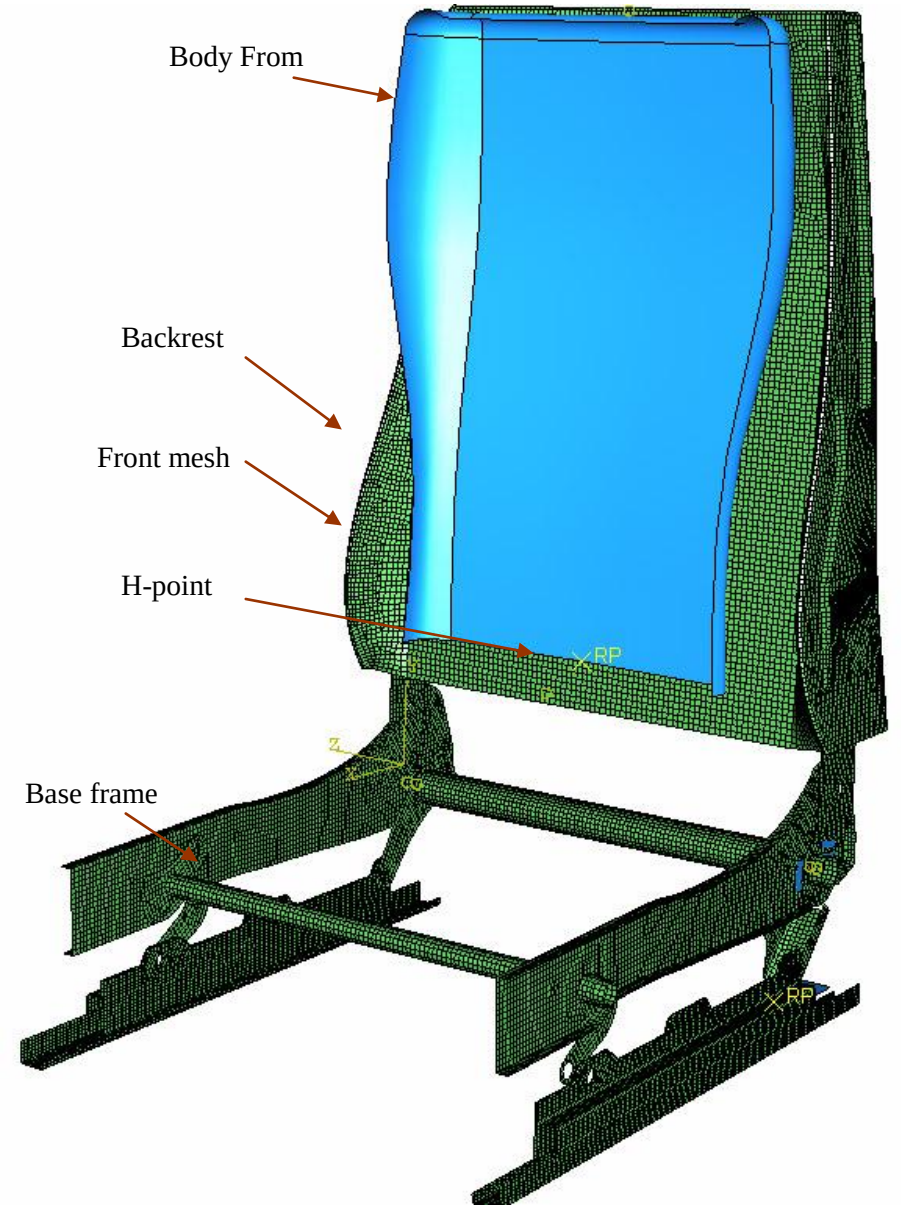

Figure 3-8: Finite Element Setup of ECE R17 Rear Impact Moment Test (Constant Angular Velocity)

The body form is rotated about the H-point axis with a constant angular velocity of ω_0 = 0.063 deg/sec. The angular velocity of the body form is low in order to eliminate the effect of inertia when the seat comes in contact with the body form thus simulating a quasi-static strength test of the seat. Initial ramp up from zero to final velocity is achieved by a smooth step function between t = 0 sec and t = 100 sec as shown in Figure 3-9. After t = 100 sec the angular velocity is kept constant for the rest of the time period until 400 sec. In ABAQUS, the smooth step amplitude function for the angular velocity is defined by a fifth order spline function

$$\omega(t) = \begin{Bmatrix} \omega_0(10 - 15\xi + 6\xi^2)\xi^3 & , \quad 0 \le t \le 100\,\text{sec} \\ \omega_0 & , \quad 100 \le t \le 400\,\text{sec} \end{Bmatrix} \qquad (3\text{-}3)$$

where $\xi = t/100$ is the normalized time, ω_0 = 0.063 deg/sec is the constant angular velocity and t is time measured in seconds.

The constant angular velocity input to the body form rotates the body form about the H-point axis of the seat. The deflection of the seat is measured by the angle θ with which the body form rotates from initial position at t = 0 sec to final position at t = 400 sec. The angular displacement is defined by the integral of the angular velocity over the time interval.

$$\theta(t) = \begin{Bmatrix} \omega_0((5/2)\xi^3 - 3\xi^4 + \xi^6), 0 \le t \le 100\,\text{sec} \\ \omega_0\ \xi \qquad\qquad\qquad\qquad , 100 \le t \le 400\,\text{sec} \end{Bmatrix} \qquad (3\text{-}4)$$

where $\xi = t/100$ is the normalized time, ω_0 = 0.063 deg/sec is the input angular velocity, t is the time measured in seconds and $\theta(t)$ is the angular rotation of body form.

As shown in Figure 3-10 and Figure 3-11, the amplitude function for angular displacement and angular acceleration of the body form are plotted over the entire time period from t = 0 sec to t = 400 sec. The ramp up in angular velocity causes the body form to rotate in a nonlinear fashion from 0 sec to 100 sec and remains linear from 100 sec to 400 sec. The smooth ramp up of angular velocity from 0 to 100 sec and constant over the remaining time period until 400 sec causes the angular acceleration to ramp up and then back to zero in 100 sec and the acceleration remains zero over the remaining time period from 100 sec to 400 sec.

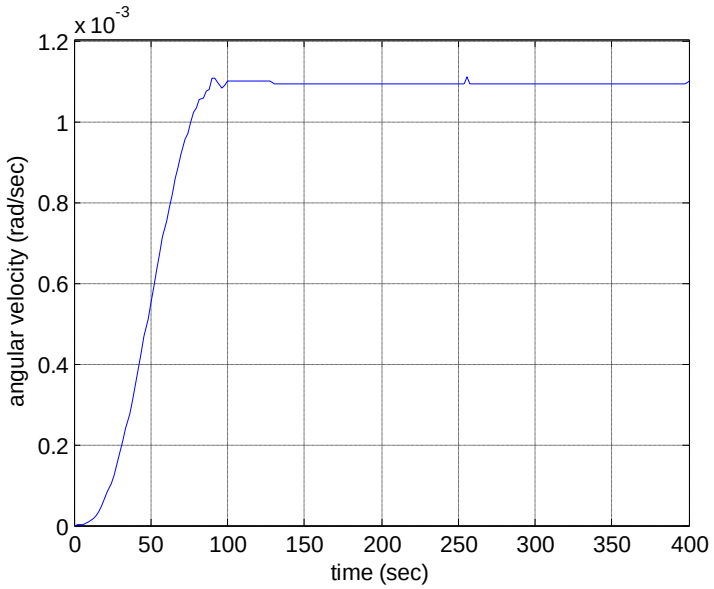

Figure 3-9: Smooth Step Amplitude Function for Angular Velocity $\omega(t)$

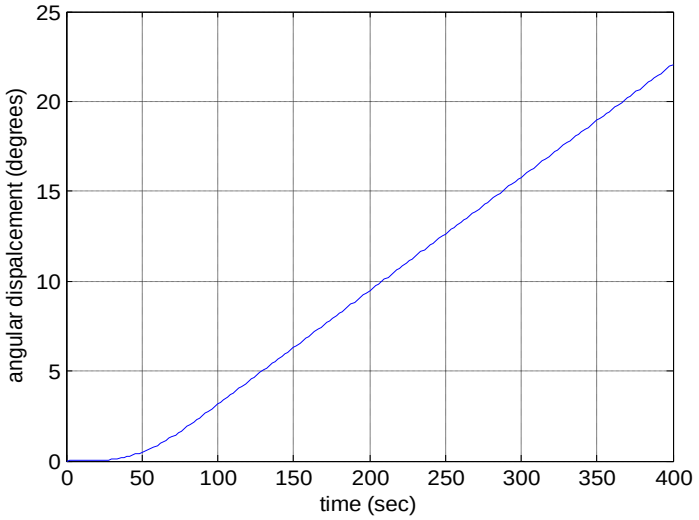

Figure 3-10 : Angular Displacement of the Body Form

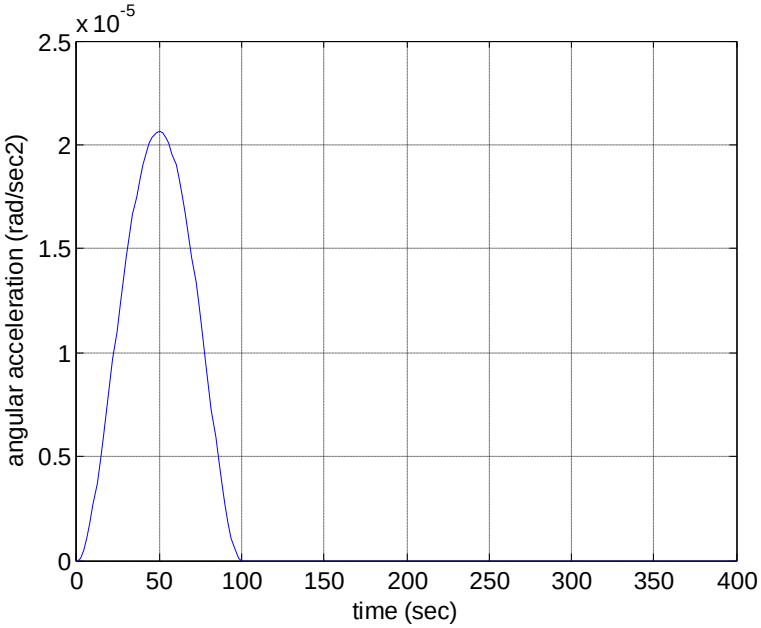

Figure 3-11: Angular Acceleration of the Body Form

The moment deflection characteristics of a seat are calculated by measuring the reaction moment at the H-point due to the angular displacement of the body form against the seat. The reaction moment M (t) and $\theta(t)$ are measured at the H-point i.e. reference point of the body form. The moment-deflection characteristic plot is obtained by plotting M(t) against $\theta(t)$.

CHAPTER 4

ELASTIC-PLASTIC MATERIAL MODEL

Finite element analyses of structural components made from ductile materials under the influence of high loads causing yielding of the material require the use of a plasticity material model. Elastic behavior of the material occurs when the strains in a material are low. The stress strain curve in the elastic region is a straight line until the proportional limit, so the stress is proportional to the strain. The proportionality constant is called modulus of elasticity which is a measure of the stiffness of the material. When the material is stressed above the elastic limit of the material, permanent deformation of the material occurs and exhibits a nonlinear relation between stress and strain. After yielding the material continues to carry load until the maximum stress reaches ultimate stress, so the stress strain curve rises to the ultimate stress but becomes flatter.

Ductile materials like metals have the ability to withstand loads causing large strains without failure in the material. Ductile materials are used extensively in the design of automotive structures because they are capable of exhibiting large deformations before failing. The ductility of a material is measured by the percentage elongation of the specimen before failure [13]. In the elastic region, materials have linear behavior with a slope defined by Young's modulus as shown in the Figure 4-1. Young's modulus defines slope of the stress-strain curve in the elastic region of a material.

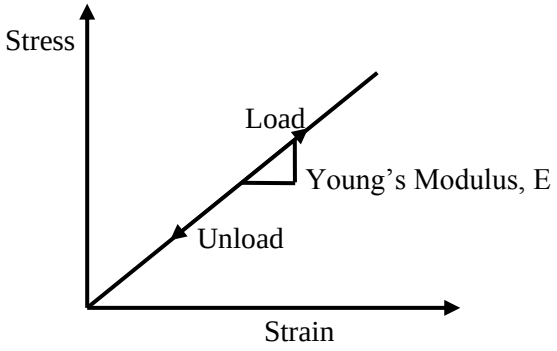

Figure 4-1: Stress - Strain Behavior of a Linear Elastic Material

During tensile test loading, measures of true stress and true strain for the material is defined by

$$\varepsilon = \int_{l_o}^{l} \frac{ds}{s} = \ln(\frac{l}{l_0}) \qquad (4\text{-}1)$$

where ε is the true strain, l is the length after deformation and l_0 is the original length. The true stress σ is defined by

$$\sigma = F / A \qquad (4\text{-}2)$$

where F is the normal force in the material and A is the current area of cross section.

Plastic behavior of materials occurs beyond the yield point, causing permanent deformation of the material. Often ductile materials such as steel exhibit hardening in which stiffness increases with increased strain beyond the yield point. The strains associated with the permanent deformation are called plastic strains. In the plastic region the total strain of a material

is considered as the sum of recoverable elastic strain and permanent plastic strain components as shown,

$$\varepsilon = \varepsilon^{el} + \varepsilon^{pl} \tag{4-3}$$

where ε is the total true strain in the material, ε^{el} is the elastic strain in the material and ε^{pl} is the plastic strain in the material.

The test specimen data provide the nominal stress and nominal strain of a material as the original cross-sectional area and length are considered to calculate the stress and strain instead of using the actual cross-sectional area and length at the instance of measuring load. For ductile materials such as steel, after yielding, the material can carry load and the stress strain curve becomes flatter until ultimate tensile load is reached. Finally, necking occurs in a material before it yields considerably and fails during which time the original length and cross-sectional area change dramatically [13].

Plasticity material models in ABAQUS require true stress and plastic strain as inputs [14]. The plastic material test data should be converted from nominal stress/strain values to true stress/strain values [15]. The relation between true and nominal stress is formed by considering the incompressible nature of the plastic deformation and then forming an expression relating the current area of cross-section to the original area of cross-section, i.e.

$$l_0 \, A_0 = l \, A \qquad or \qquad A = A_0 \frac{l_0}{l} \tag{4-4}$$

where l_0 is the original length, A_0 is the original area of cross-section, l is the current length, and A is the current area of cross-section.

The current area of cross section A is substituted in the equation for true stress (4-2) in order to obtain a relationship between true stress and nominal stress,

$$\sigma = \frac{F}{A} = \frac{Fl}{A_0 l_0} = \sigma_{nom}\left(\frac{l}{l_0}\right) = \sigma_{nom}\ 1+\varepsilon_{nom} \tag{4-5}$$

where σ is the true stress, $\sigma_{nom} = \frac{F}{A_o}$ is the nominal stress, and $\varepsilon_{nom} = \left(\frac{l - l_0}{l_0}\right)$ is the nominal strain. Using the result $\varepsilon_{nom} + 1 = l / l_0$ and using (4-1), the relationship between the true strain and the nominal strain is

$$\varepsilon = \ln\ 1+\varepsilon_{nom} \tag{4-6}$$

where ε is the true strain defined by equation (4-1)

The true strain of a material from test data is a sum of plastic and elastic strain. ABAQUS requires an input of the plastic strain component of the material. The component of plastic strain is calculated by subtracting the component of elastic strain defined as the value of true stress divided by Young's modulus, from the total strain as shown below

$$\varepsilon^{pl} = \varepsilon - \varepsilon^{el} = \varepsilon - \left(\frac{\sigma}{E}\right) \tag{4-7}$$

where ε is the total strain in the material, ε^{el} is the elastic strain in the material, ε^{pl} is the plastic strain in the material, σ is the true stress, and E is the Young's modulus for the material.

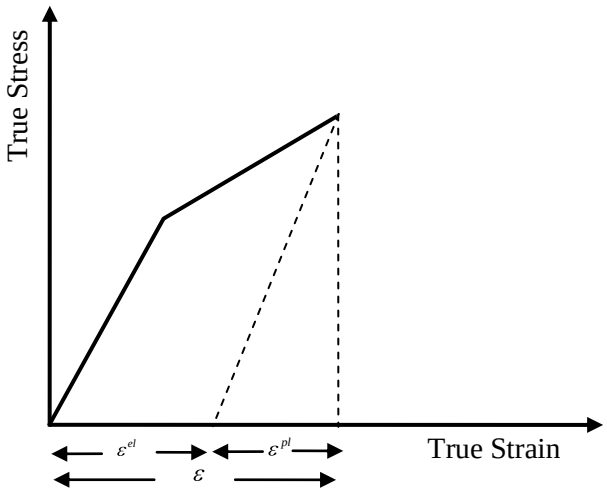

Figure 4-2: Total Strain as a Component of Platic Strain and Elastic Strain

Different grades of steel are evaluated for material modeling in ABAQUS for the various structural components of the seat. The material properties considered are steel grades representative of typical low, medium, and high strength steels. Young's modulus is assumed 210 GPa for each grade of steel. The mass density of steel is assumed to be 7.85 g/cc with Poisson's ratio 0.29. The basic differences among the three different grades of steel considered are the yield points, ultimate tensile points and % elongation at failure measuring ductility and stretching capability. The material properties of different grades of steel considered are given in the Table 4-1.

	Low Strength Steel	Medium Strength Steel	High Strength steel
Density ρ (g/cc)	7.85	7.85	7.85
Young's modulus E (Gpa)	210	210	210
Poisson's ratio υ	.29	.29	.29
Yield Strength (MPa)	305	350	365
Ultimate Tensile Strength (MPa)	365	515	635
% Elongation at break	20	30	24

Table 4-1: Material Property Chart for Different Grades of Steel

		Low Strength Steel	Medium Strength Steel	High Strength Steel
True stress	Yield strength	305	350	365
	Ultimate tensile Strength	438	669.5	787.4
True strain	Initial strain	0	0	0
	Strain at failure	0.182	0.2623	0.215
Plastic strain	Initial Plastic strain	0	0	0
	Plastic Strain at failure	.18	0.262	0.212

Table 4-2: Stress - Strain Input Data to ABAQUS for Different Grades of Steel

ABAQUS interpolates linearly between the material data points of true stress and plastic strain to produce a piecewise linear stress-strain curve for the plastic strain with hardening [16]. An isotropic hardening rule is selected in ABAQUS to model loading and unloading of the stress-strain curve. The stress outside the range of data points is assumed to be constant in order to restrict the stress to the ultimate tensile strength. Figure 4-3 shows the piecewise linear plastic model for medium strength steel. The plastic strain at yield stress is zero and reaches a maximum of 0.262 at ultimate tensile strength. Plastic strain greater than or equal to 0.262 is considered failure.

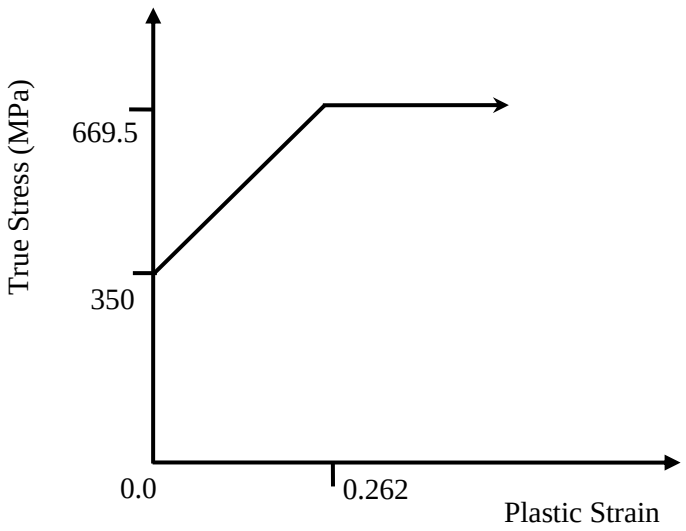

Figure 4-3 : ABAQUS Input Data for Elasto-Plastic Material Behavior

CHAPTER 5

FINITE ELEMENT MODEL OF REFERENCE AUTOMOTIVE FRONT SEAT

5.1 Geometric Modeling of the Reference Seat

A geometric model is used to represent the physical seat. The geometric modeling of the seat is carried out in the Computer-Aided Engineering software I-DEAS which is capable of producing precise solid and surface geometry. Finite element models associated with the geometric model of the seat are created in order to analyze the strength of the seat. Surface geometry is used to represent the seat components because the structural members are manufactured by forming sheet metal. The dimensions of the reference seat were measured a close representation of the important geometric parameters to the physical seat are modeled. Detailed surface models of the major seat structural members including the backrest, connector, base frame and slider rails which are the major load bearing components were drawn in I-DEAS, see Figure 5-1. Appropriate measured thicknesses were associated to different surfaces of the geometric model.

The stamping features on the backrest vertical members like bends and fillets are represented in the geometric model, including an approximation to the sleeve pockets and support structure on the vertical members for attaching the connectors. The additional stiffness to the backrest obtained by welding the support structure is approximated by increasing the thickness at locations of the backrest where the support structure is attached. The backrest pivot on the base frame which is reinforced with extra sheet metal structure for support is approximated by increasing the thickness in the geometric model at the pivot point. The short continuous welds at different locations on the backrest are approximated by complete continuous welds by stitching surfaces together.

A polymeric mesh is used to approximate the resting surface on the backrest. Contours of the side bolster area of the resting surface were modeled to accurately represent the load path. The polymeric front mesh is assumed to have a density of 3.5g/cc with linear elastic material model with Young's modulus of 20 GPa and Poison's ratio of 0.35. This material model for the resting surface is an approximation to the PUR foam material and fabric which covers the physical seat. A detailed model of the PUR foam material is considered outside the scope of this work and is suggested for future studies. From the results of simulations, the material parameters used in this study provided a good approximation to the compliance of the seating surface.

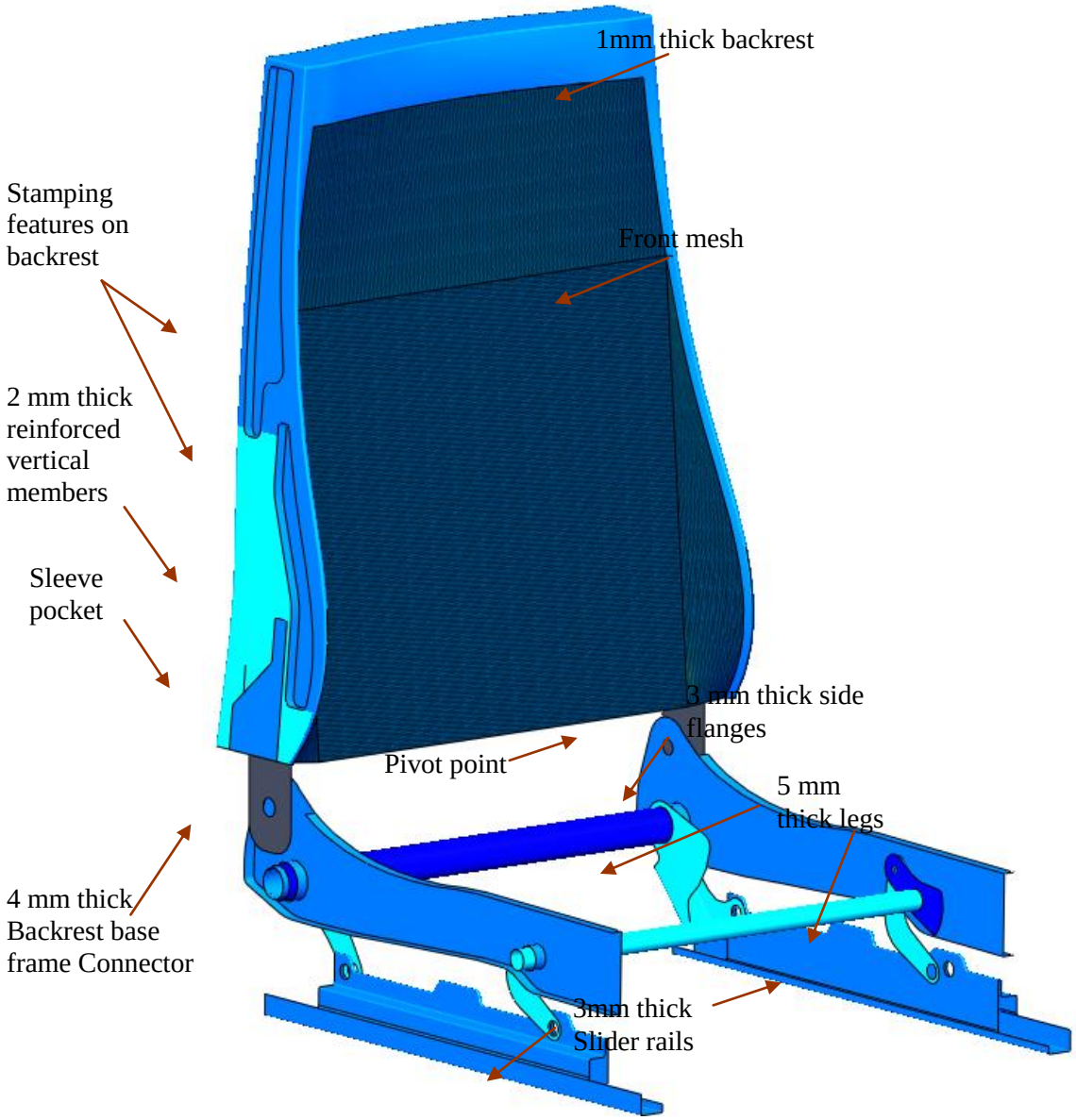

Figure 5-1: Geometric Model of Reference Seat

5.2 Meshing Geometric Seat Model

The surfaces of the geometric CAD model generated in I-DEAS are meshed using shell elements to represent the relatively thin sheet metal structures of the seat. Four node quadrilateral elements of type S4R with seed size of 4 mm have been generated for all the surfaces using the

free meshing tool in I-DEAS. Triangular elements of type S3R are also allowed in the finite element mesh in order to allow good mesh quality. The entire seat model contains 39975 nodes and 39247 elements out of which 37852 are quadrilateral elements and 1395 are triangular elements. Each node has displacement components and rotational degrees of freedom. Quality checks are made in order to eliminate coincident nodes and coincident elements. A standard mesh sensitivity analysis is carried out in order to ensure that the results obtained are effectively insensitive to the size of the elements used. The finite element shell mesh generated in I-DEAS is exported to ABAQUS for further model definition and analysis. The rigid surface representing the body form is meshed with rigid elements of type R3D4 in ABAQUS.

5.3 Contact Modeling for Simulating ECE R17

ABAQUS/Explicit allows self contact between parts in the model. Contact modeling is used to simulate the interaction between parts in the seat which may bear against each other during deformation under load. Separation of surfaces is allowed after two parts come in contact during an analysis. Contact is also defined for the rigid body form coming in contact with the deformable back rest. Contact within the seat structure is defined in order to simulate joints between side flanges and cross tube members. Contact also occurs between the backrest tilt adjustment locking tube located inside the rear outer tube. Figure 5-2 shows the location of contact regions between the base frame flanges and cross-tubes.

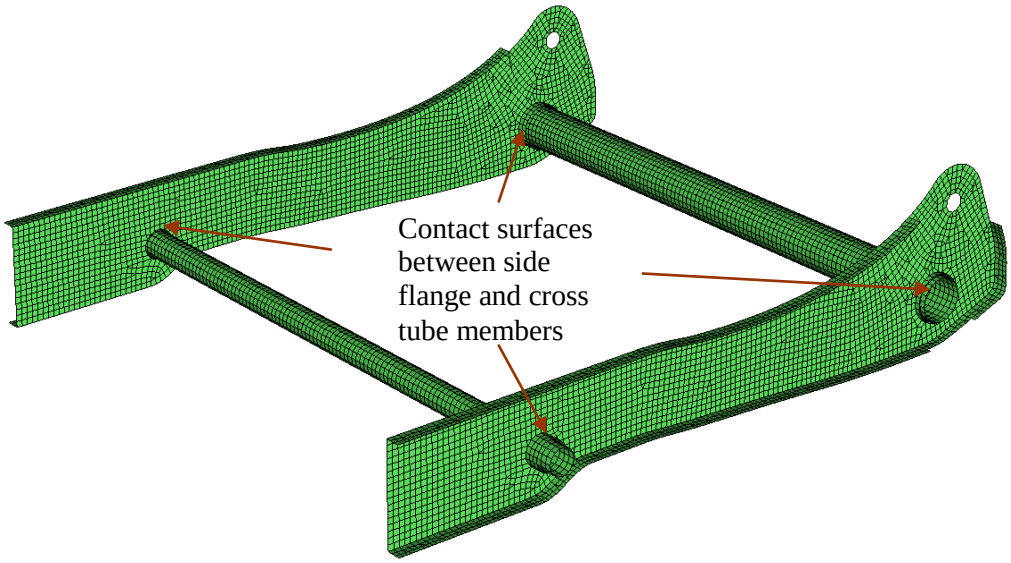

Figure 5-2: Contact Modeling Between Side Flanges and Cross Tube Members

5.4 Multi-Point Constraints for Modeling Seat Joints and Mechanisms

Multi-point constraints have been used to connect the different locking mechanisms and joints in the seat. The seat has bolt connections at different locations and mechanisms involving cams and gears in order to lock and unlock height, front tilt, and back rest angle adjustments. The seat has a total of 8 bolt connections. Four bolt connections exist between the four legs and slider rails, two between the front legs and tilt gears on both sides, and two between the side flanges of the base frame and backrest to base frame connector plate. Rigid connectors have been used to create bolt connections. All the nodes on the edge of a hole are constrained in all six degrees of freedom to a point representing the center of the hole using couplings in ABAQUS. The center points of holes on the two surfaces bolted together are connected by a rigid link with all degrees of freedom constrained except for rotation about axis of the link. This multi-point constraint simulates a pin jointed bolt connection. Figure 5-3 shows the model of the pin jointed bolt connection between a front leg and slider rail modeled using multi-point constraints.

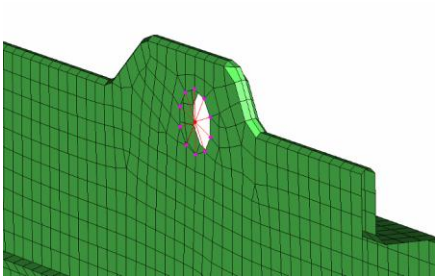

(a)

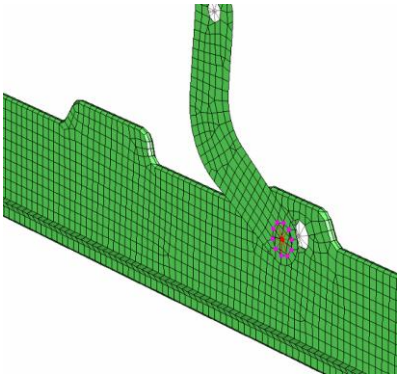

(b)

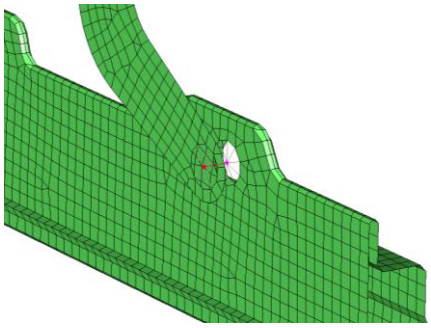

(c)

Figure 5-3: (a) Multi-point constraint on slider rail (b) Multi point constraint on front leg (c) Rigid link connecting front leg and slider rail representing a bolt connection.

The mechanisms used to lock the backrest tilt angle, height adjustment, and front tilt are represented in the finite element model using rigid links. The backrest base frame connector pivots about a point on the side flange and meshes with the small gear on the inner rod passing through the back tube. The back rest tilt gear located on the inner rod is locked to the side flange on the door side by the back rest tilt mechanism. The back rest tilt lock is represented in the finite element model by connecting rigid body links with z- displacement (lateral direction) constraint released between the bottom edge of the connector and the small gear on the inner rod of the backrest tilt mechanism. The large gear on the inner rod is connected to the side flange by rigid links projected to a patch of nodes on the side flange representing back rest tilt lock mechanism. Figure 5-4 shows the finite element model of backrest tilt mechanism and locking connectors.

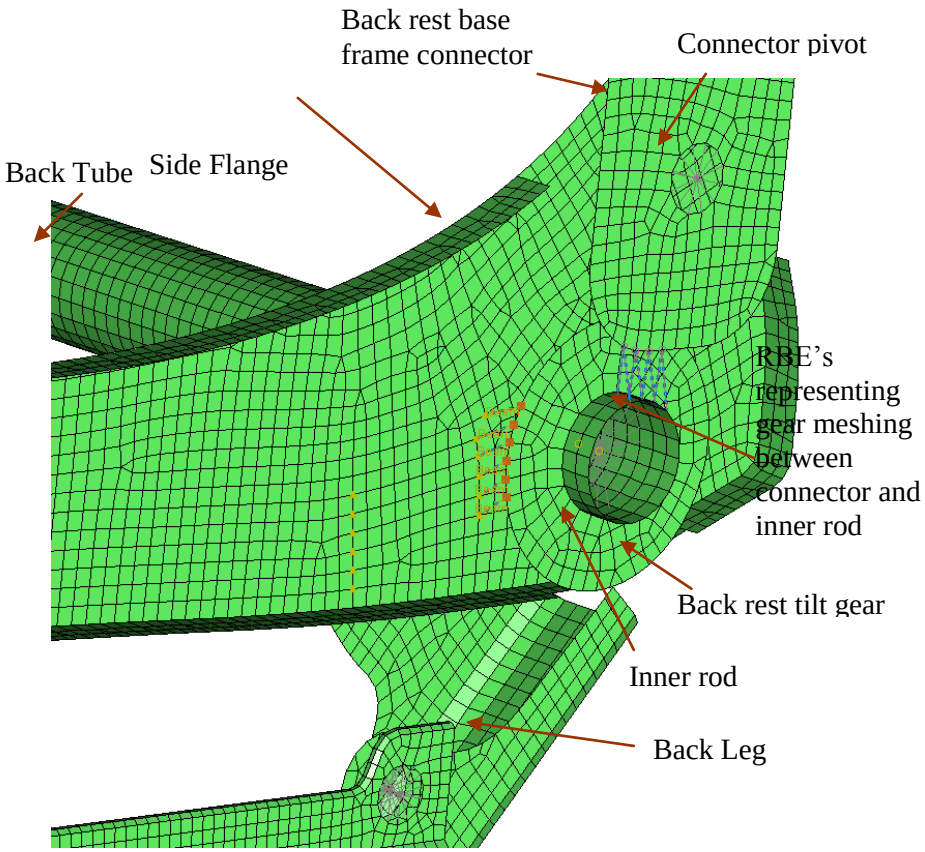

Figure 5-4: Finite Element Model of Backrest Tilt Mechanism

Rigid body elements are also used to represent the height adjustment mechanism and front tilt mechanism. Rigid body elements from the height gear and tilt gear are connected to a patch of nodes on the side flange by rigid body links to represent locking mechanisms as shown in Figure 5-5: Finite Element Model of (Left) Height Gear Mechanism, (Right) Tilt Gear Mechanism

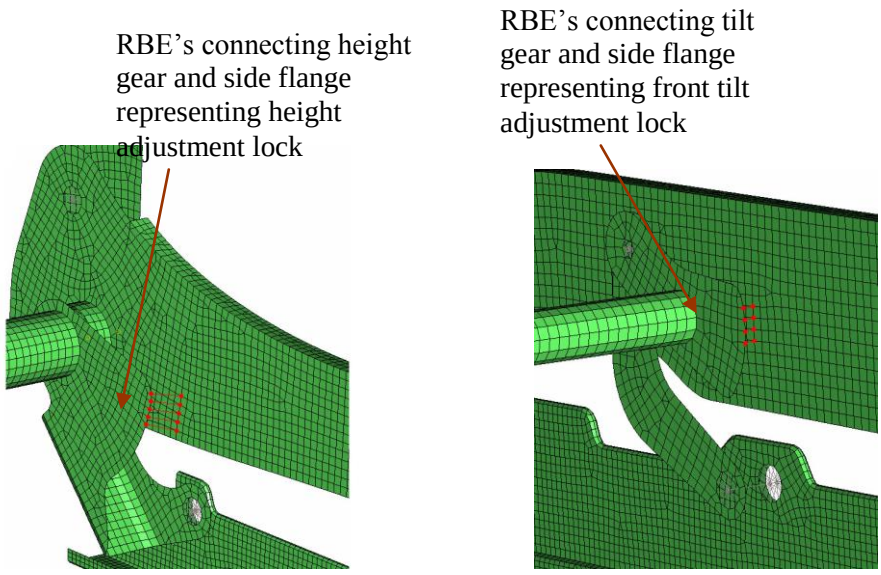

Figure 5-5: Finite Element Model of (Left) Height Gear Mechanism, (Right) Tilt Gear Mechanism

In the physical seat, the relative motion between the side flange and the back tube cross member is constrained along the axis of the tube by collar in order to prevent the sliding of side flanges over back tube. To represent this constraint in the model, as shown in Figure 5-6, the nodes on the circular edge of the back tube are constrained to a center point along the axis of the tube in all six degrees of freedom. A similar rigid wheel is created between the nodes on the circular edge of the side flange and a center point along the axis of the tube. The center points of the back tube and side flange edges are connected by a rigid link connecting their motion along the axis of the tube. Figure 5-6 shows the multi-point constraints used to constrain the relative sliding between the side flange and the back tube.

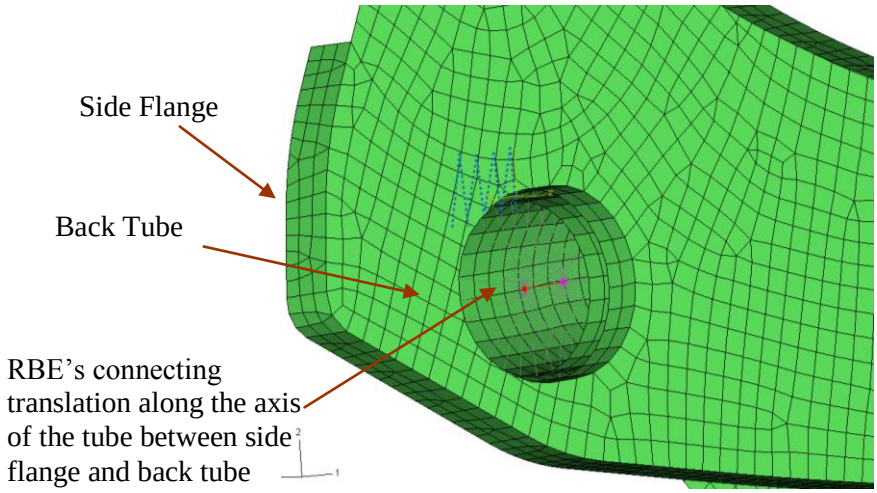

Figure 5-6: Relative Sliding of the Side Flange With Respect to Back Tube Constrained Using Multi Point Constraints.

In ABAQUS, tie nodes intended for tying different meshes together are another option which can also be used to lock height, front tilt, and backrest angle adjustments. Using the tie node feature in ABAQUS, the nodes on the edge of the adjustment gear are tied to a set of nodes on the side flange similar to rigid connectors. It was found that for all moment load simulations tested, the use of rigid connectors and tie nodes to model the locking mechanisms gave similar results. In the following studies, the rigid connectors were used for all locking mechanisms. Figure 5-7 show the finite element model of the height adjustment lock using tie nodes to connect meshes.

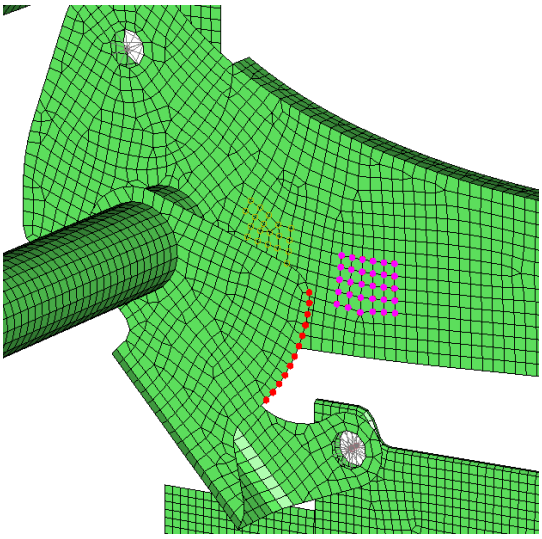

Figure 5-7: Finite Element Model of Height Adjustment Lock Using Tie Nodes to Connect Meshes.

The backrest base frame connector is located in the sleeve pocket of the backrest. The connector matches the profile of the sleeve pocket with a small gap. The backrest when loaded is supported by the connector because of the contact bearing support. Tie nodes represent the bearing contact between edges of the connector plate and surface of the pocket sleeve. Adaptive contact surface interaction models under deformation are not used due to the difficulty of representing a contact surface over the edge of shell elements modeling the connector. Figure 5-8 shows the tie nodes representing bearing contact between connector and sleeve pocket.

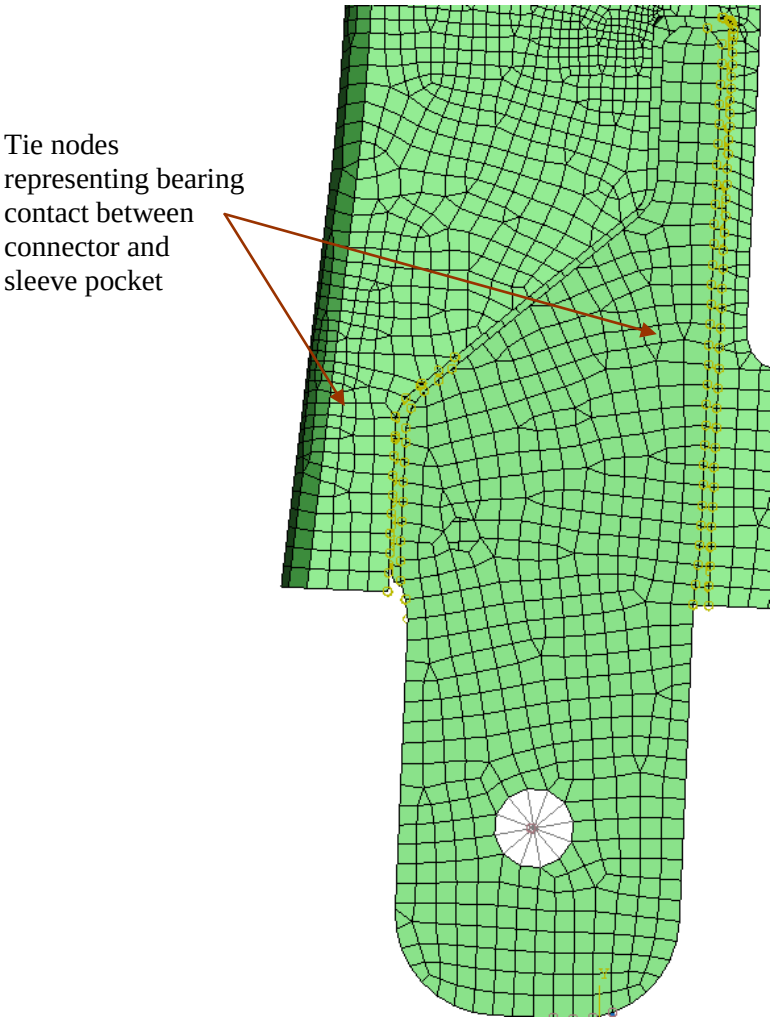

Figure 5-8 Tie Nodes Represent Bearing Contact between Connector and Sleeve Pocket.

5.5 Boundary Conditions for Reference Front Seat

The seat is attached to the floor of an automobile at the slider rails. Bolts at four different locations of the slider rails are used to restrain the seat to floor. The nodes located at the bolt connections are constrained in all 6 degrees-of-freedom at the bolt locations. Figure 5-9 shows the boundary conditions on the finite element reference seat model.

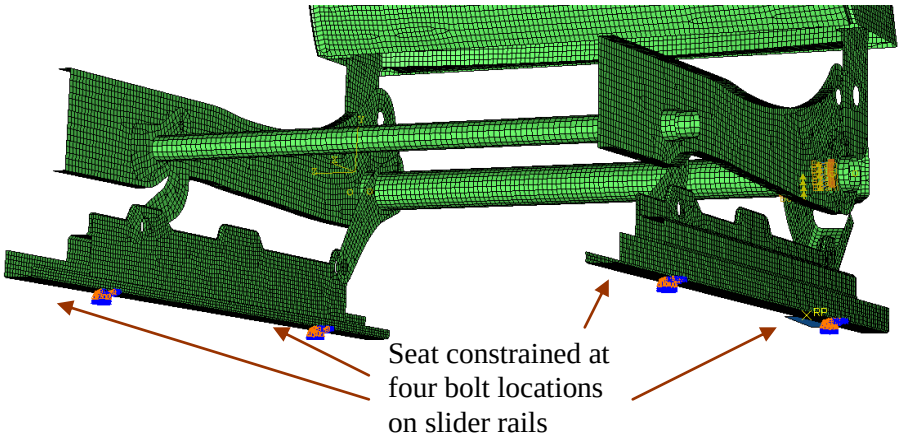

Figure 5-9 Boundary conditions on reference front seat

5.6 Explicit Dynamic Procedure

ABAQUS/Explicit has been used to evaluate the finite element model of the reference seat for quasi-static loads. ABAQUS/Explicit uses a central difference rule to integrate equations of motion in explicit dynamic analysis [15]. The equations of motion for the finite element degrees of freedom are solved for acceleration at the beginning of the current time increment using

$$\ddot{u}_{(t)} = M^{-1}(P_{(t)} - I_{(t)}) \qquad (5\text{-}1)$$

where M is the diagonal element system mass matrix, P is the applied load vector, and I is the internal force vector which is nonlinearly dependent on the displacements u.

Since the mass matrix is diagonal, the equations of the system are uncoupled so they can be solved explicitly. This makes ABAQUS/Explicit highly efficient for large deformation and nonlinear dynamic problems where small time steps are required for accuracy. Explicit dynamic

solution is advantageous because it solves each time increment without iterations and does not require the tangent stiffness matrix to be formed from the nonlinear internal force vector.

The increment in velocity is calculated based on a central difference formula for the time derivative centered at time t and assumes constant acceleration. The difference is taken over the half time step from the previous time step $t-\Delta t/2$ to the current half time step $t+\Delta t/2$ .The velocity at the middle of the current time step is updated from

$$\dot{u}_{(t+\Delta t/2)} = \dot{u}_{(t-\Delta t/2)} + \frac{\Delta t|_{(t+\Delta t)} + \Delta t|_{\Delta t}}{2} \ddot{u}_{(t)} \tag{5-2}$$

where $\dot{u}$ is the velocity, $\ddot{u}$ is the acceleration, and Δt is the time increment.

The velocities are then integrated over time based on the difference centered at $t+\Delta t/2$ and added to the displacements at the beginning of the time step t to get the displacements at the end of the time step $t+\Delta t$ from

$$u_{(t+\Delta t)} = u_{(t)} + \Delta t|_{(t+\Delta t)} \dot{u}_{(t+\Delta t/2)} \tag{5-3}$$

where $\dot{u}$ is the velocity, u is the displacement, and Δt is the time increment of the current step.

5.6.1 Stability Time Increment

ABAQUS/Explicit automatically calculates the default time increment for a finite element model to ensure sufficient stability [15]. The stable time increment for explicit dynamic method is given by

$$\Delta t = L^e / C^d \qquad (5\text{-}4)$$

where L^e is the length of the smallest element in the model, C^d is the velocity of an elastic wave defined by

$$C^d = \sqrt{E/\rho} \qquad (5\text{-}5)$$

where E is Young's modulus of the material and ρ is the mass density of the material.

When using ABAQUS/Explicit, the length of the element in a finite element model should be relatively uniform through out the model for efficiency. Mesh non uniformity and poor quality will decrease the stable time increment thus increasing the number of iterations required to solve a problem. The smallest element in the model controls the time increment of explicit dynamic method in ABAQUS/Explicit. The finite element model for the reference seat has a smallest element length of 2 mm in the fillet region. The density of steel in the model is 7.85 e-9 ton/cubic millimeters with Young's modulus of 2.1e5MPa, therefore the stable time increment calculated from (5-4) for the model is 3.885e-7sec. The automatic value used by ABAQUS/Explicit was very close to this value.

5.7 Quasi-Static Simulation in ABAQUS/Explicit

ABAQUS/Explicit has been used to model the quasi static moment test on a seat in rear impact according to ECE R17. To be considered quasi static analysis the kinetic energy of the model should be less than 5% of the internal energy of the whole model through out the simulation [17]. If a model has low kinetic energy compared to the internal energy the inertia forces are small. Mass scaling is used to increase the solution time by changing the material

density which in turn increases the stable time increment. To ensure that accuracy is not lost and the quasi-static mass inertia forces are negligible the kinetic energy was calculated and compared to the total internal energy. Figure 5-10 shows energy results for the moment test simulated with constant angular velocity. The analysis is considered quasi-static, since the kinetic energy of the model is below 5% of the internal energy over the entire time period of the event.

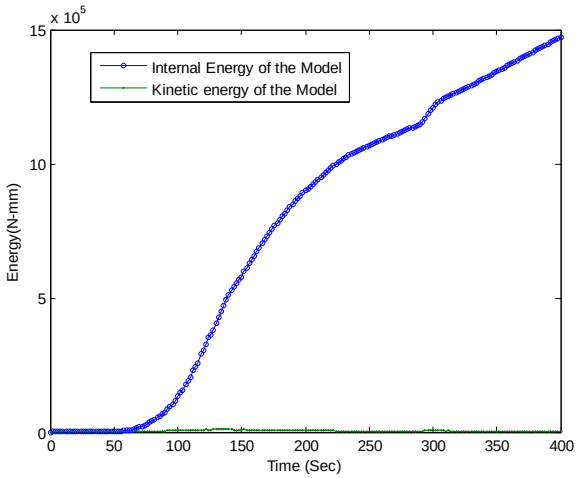

Figure 5-10: Comparison of Kinetic Energy and Internal Energy of the Model.

CHAPTER 6

RESULTS FROM FINITE ELEMENT SIMULATION OF MOMENT TEST

ABAQUS/Explicit is used to simulate the quasi-static rear impact test on the finite element reference seat model. The finite element simulation of the quasi-static rear impact test for a reference automotive front seat is carried out as described in ECE R17 Section 6.2. The reference seat is tested in order to predict the moment-deflection characteristics developed during the quasi-static rear impact test. Two complementary loading models for simulating the backrest moment test are considered as discussed earlier in Chapter 3. In the first set of simulations, a constant horizontal force is applied to the reference point on the rigid body form. In the second study, a constant angular velocity of the body form is considered. Validation and correlation of the finite element predictions with a physical test was not possible as test data is not available.

6.1 Simulation of Moment Test (Constant Horizontal Force)

This section, discusses the simulation of the moment test using a constant horizontal force, as described in Section 3.2 1, is simulated for the reference seat finite element model. The finite element model of the reference automotive seat associated with the geometric model is used to simulate the moment test. The overall dimensions and thickness of the different surfaces of the finite element model were summarized earlier in Chapter 5. Material properties representing typical low, medium, and high strength steel grades are taken from Table 4-1. The seat is modeled at nominal riding position with backrest at 25 degrees torso angle and height adjustment at 35 mm. The backrest and base frame are modeled as low carbon and medium carbon steel, respectively. The 4 mm thick backrest to base frame connector plate is made of high-strength steel with increased ultimate strength because it is a major load bearing component transferring the load on from the back rest to the base frame. The SAE J826 rigid body form along with the rigid link is free to rotate about H-point. The rigid link between H-point and reference point of the

body form constrains all degrees of freedom except rotation about the H-point axis. As a result, the body form can independently rotate about the reference point. The horizontal force applied at the reference point causes the body form to initially make contact with the front mesh and backrest top cross member. Since the body form is free to rotate about the reference point, after a short amount of time, it establishes uniform contact over the entire front mesh. The highest stress values developed during the moment test on the backrest are located on the vertical members where the cross-sections transition from wide at the bottom to narrow at the top and side bolster region of the backrest. The high stress of 320 MPa on the backrest is slightly above the yield of value of 305 MPa, but well below the ultimate strength for low strength steel. The side flanges of the base frame are subjected to bending because of the locking forces from the adjustment mechanisms. Of the four legs, the back leg on the door side yields first causing it to deform and rock the base frame back slightly until the flat stop region of the back leg makes contact on the slider rail.

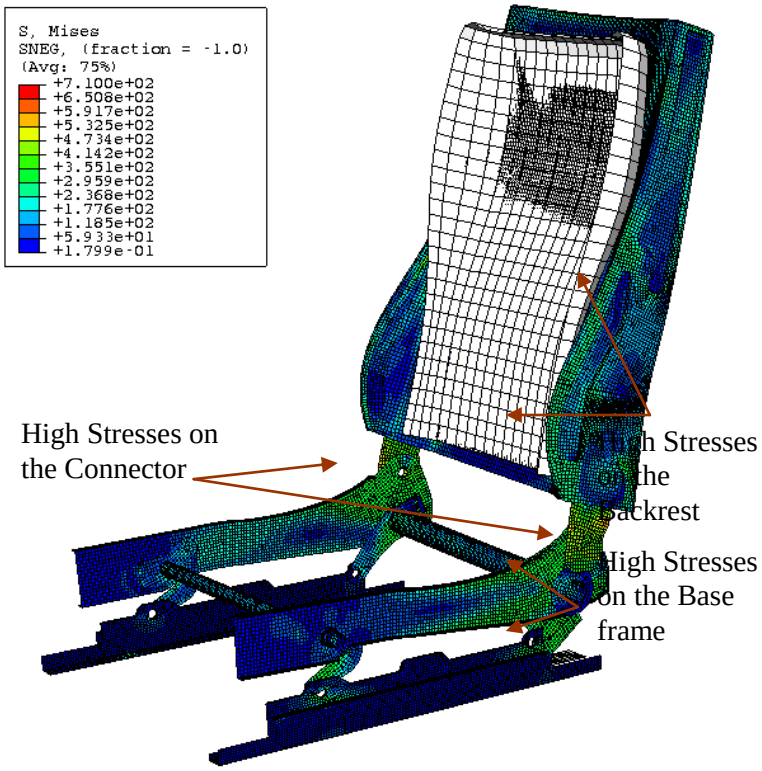

Figure 6-1: Contours of Von-Mises Stress for Moment Test (Constant Horizontal Force) at Maximum Developed Moment.

Figure 6-1 shows contours of Von-Mises stress when the developed moment about the H-point reaches a maximum value just above M_0. The backrest base frame connector has a maximum stress of 630 MPa well above the yield value of 365 MPa, yet below the true failure stress value of 787.4 MPa for high strength steel. The connector deforms while transferring load from backrest to the base frame changing the angle of the backrest with respect to the base frame. The load from the connector is transferred to the side flanges of the base frame through the pivot point and the backrest tilt adjustment mechanism. The load transferred to the pivot point of the side flanges from the connectors causes a high stress of 390 MPa surrounding the pivot point, which is beyond the yield point of medium strength steel used for the base frame.

Figure 6-2 shows the in-plane principal plastic strain in the reference seat model. The maximum plastic principal strain of 0.005 in the backrest is located on the transition region from wide at the bottom to narrow at the top. The maximum stain of 0.02 in the base frame is located on the door side leg and pivot point region. The maximum strain in the connector is 0.08.

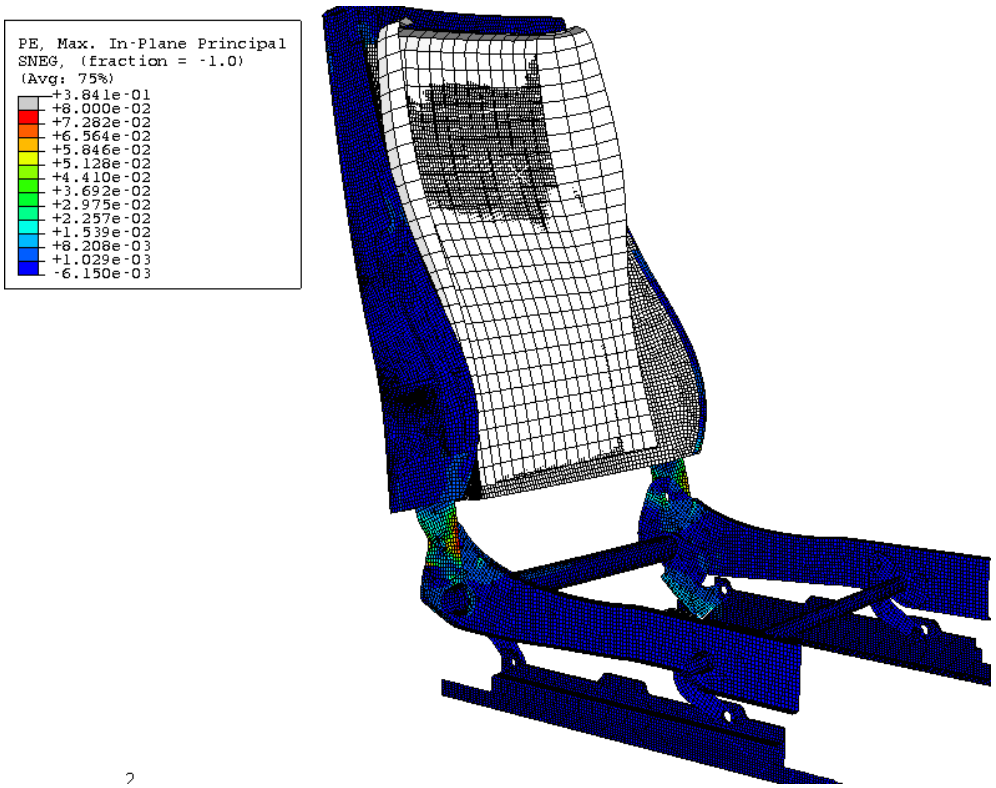

Figure 6-2: Plastic Strain in the Reference Seat Model

Figure 6-3 shows the developed moment about the H-point versus change in torso angle and shows the force exerted by the body form on the backrest deforms the seat through a torso angle in a controlled manner. The moment developed in the simulation is normalized with respect to M_0. Results from the simulation show that the reference front seat considered supports a normalized moment of 1 at the intermediate torso angle and maintains above the minimum

required normalized moment of 0.56 at the end of deformation travel, as required by the test requirements.

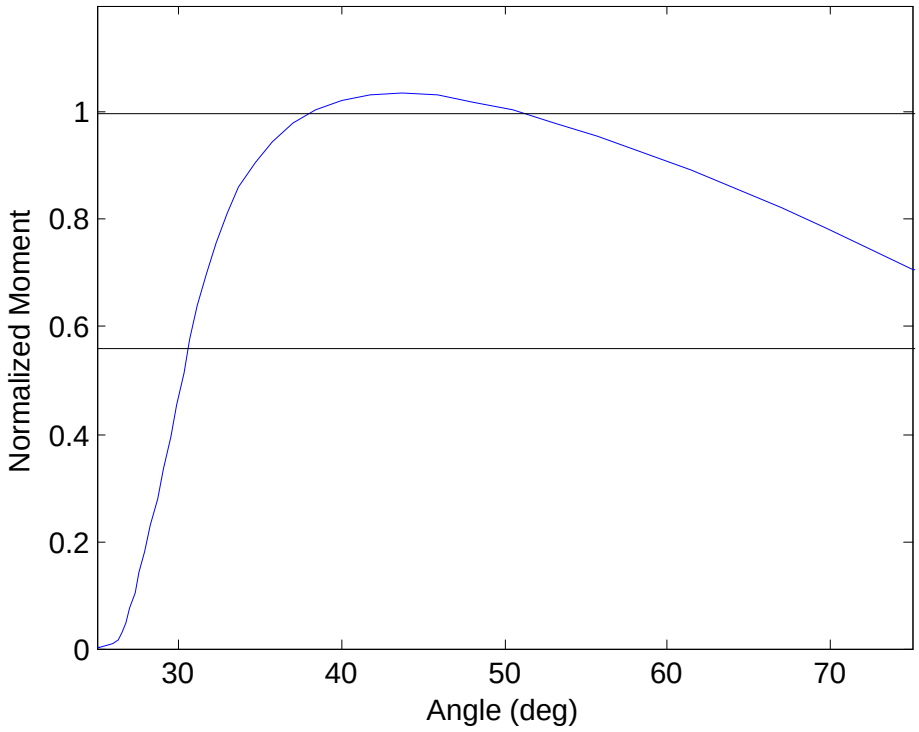

Figure 6-3: Moment vs. Torso Angle for Moment Test (Constant Horizontal Force).

6.2 Simulation of Moment Test (Constant Angular Velocity)

In this section the quasi-static moment test is simulated using an input constant angular velocity for the torso angle of the reference automotive front seat as described earlier in Section 3.2.2. The reference point located at the bottom edge of the body form is aligned with the H-point axis of the seat and an angular velocity boundary condition is provided at the reference point of the body form. The reaction moment at the reference point of the body form due to resistance of the seat is measured. The moment deflection characteristics are obtained by plotting the reaction

moment at the H-point against angular displacement of the body form. The body form is constrained at the reference point in all direction except for rotation about the H-point axis. In this simulation the body form initially contacts the top cross member of the backrest. The displacement of the seat is enforced by the body form rotation about the H-point axis.

Figure 6-4 shows contours of Von Mises Stress on the reference front seat after 25 degrees rotation. The maximum Von Mises stress of 607 MPa is above the yield point for high strength steel and is located on the connector. The region of high stress on the backrest is located on the transition region from wide at the bottom to narrow at the top. The high stress on the backrest is 310 MPa which is slightly above the yield point of low carbon steel. The base frame has a maximum stress of 320 MPa on the region surrounding the pivot point and is below the yield point of medium carbon steel.

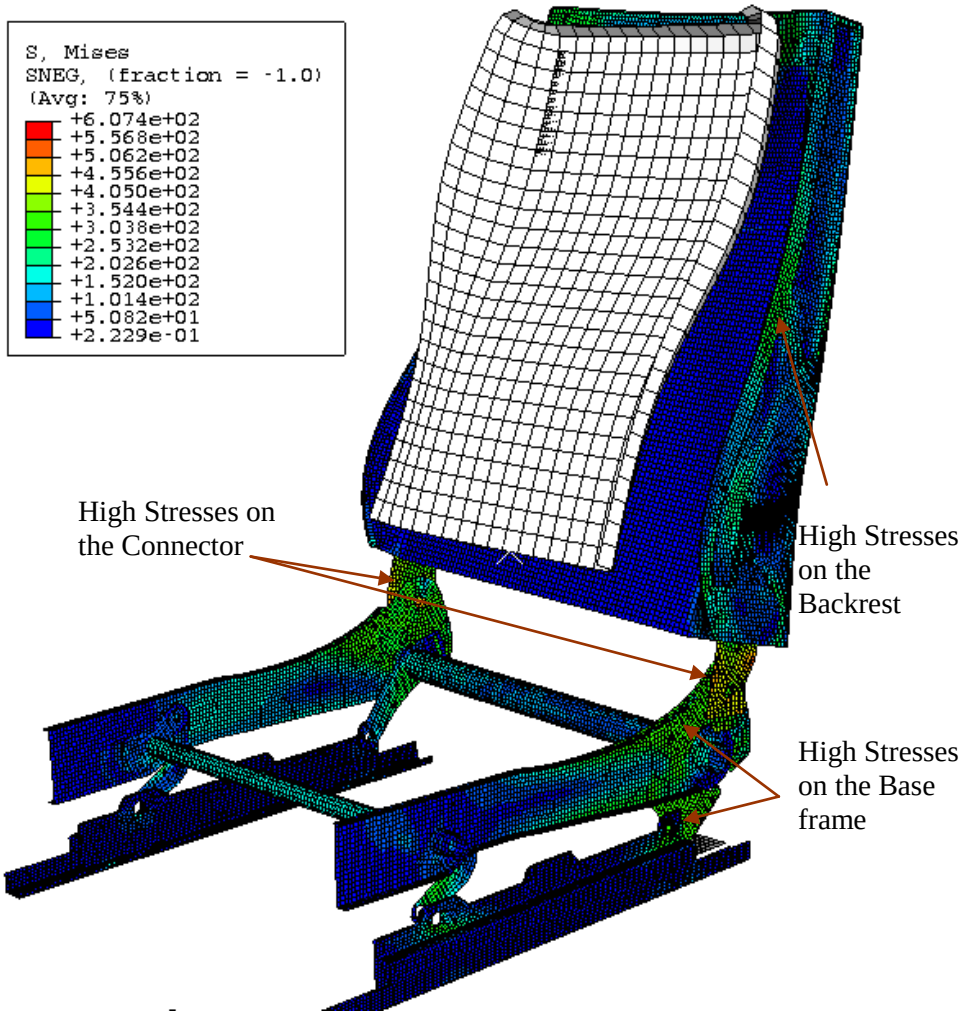

Figure 6-4: Contours of Von Mises Stress for Moment Test (Constant Angular Velocity) after 25 degrees rotation.

The results of the simulation using prescribed constant angular velocity of the body form show that the developed normalized reaction moment at the H-point maintains above the minimum required moment of $0.56\,M_0$ throughout the deformation of the seat. The reaction moment developed in the simulation is normalized with respect to M_0. The moment developed at the H-point of the seat obtained from the moment test simulated with constant angular velocity does not reach the maximum M_0 N-m limit as prescribed in the horizontal force moment test

simulation. Because the rate of change of the angular displacement of the body form in contact with the seat is held constant, the seat is forced to conform to the deformation rate of the body form. As a result, the natural development of seat deformation must continuously adjust to this constraint causing fluctuations in the moment reaction.as shown in Figure 6-5.

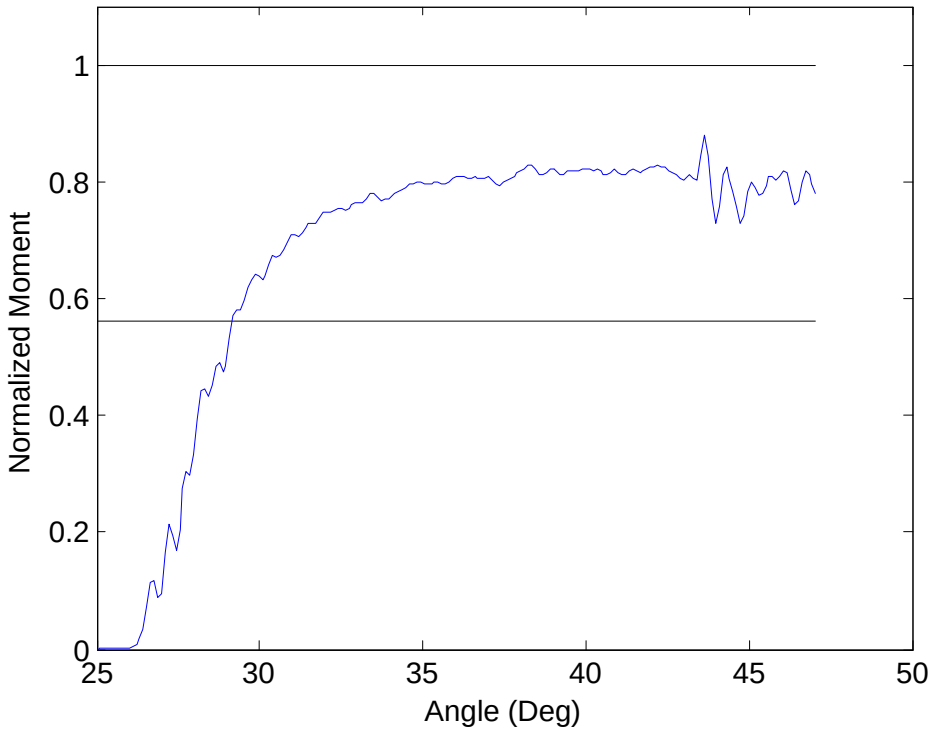

Figure 6-5 Moment Deflection Plot for Moment Test (Constant Angular Velocity)

6.3 Simulation of Moment Test (Constant Horizontal Force): without Baseframe

In this section, the moment test is simulated using a constant horizontal force with a backrest attached to the connector isolated from the base frame. The backrest and the connector are isolated from the base frame in order to understand the strength and deflection performance of the backrest together with the connector, compared to the complete model with flexible base frame. The back rest tilt lock is simulated by fixing the bottom edge of the connector. A Multi-

point constraint is created at the pivot point by connecting nodes on the circular edge of pivot point to the center by rigid links. The centers of the circular edges of pivot points are constrained except for the rotation about the axis connecting the centers of pivot points.

Using this component model of the backrest frame and connector, the high stress values developed during the moment test on the backrest occurred on the vertical members where the transitions from wide at the bottom to narrow at the top and on the region surrounding the sleeve pocket. The high stress of 315 MPa located on the backrest is slightly above the yield point of 305 MPa, but well below the ultimate strength of low strength steel. The backrest base frame connector has a maximum stress of 510 MPa well above the yield value of 365 MPa, yet below the true failure stress value of 787.4 MPa for high strength steel. Comparing to the complete model including the stiffness of the base frame, the maximum stress in the backrest does not change significantly, while the highest stress in the connector decreases from 630 MPa to 510 MPa, indicating that the flexibility of the base frame increases the strain in the connector. Figure 6-6 shows the von mises stress on the reference seat backrest with connector.

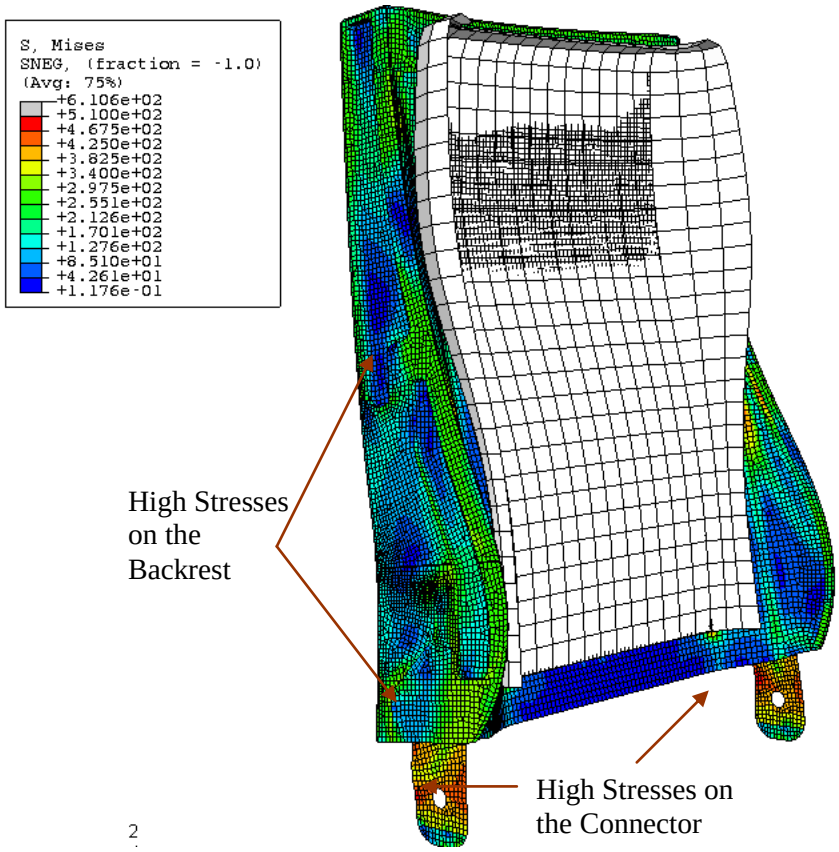

Figure 6-6: Contours of Von Mises Stress on Reference Seat Backrest with Connector for Moment Test (Constant Horizontal Force)

Figure 6-7 shows the developed moment about the H-point versus change in torso angle. Results from the simulation show that backrest with connector isolated from the base frame and rigidly restrained is stiffer than the full scale seat model and supports a normalized moment of 1 at a much larger torso angle and remains above the minimum required normalized moment of .56 as required by the test requirements. The component backrest and connector model is able to develop a higher moment than the complete seat model because does not account for the flexibility of the base frame.

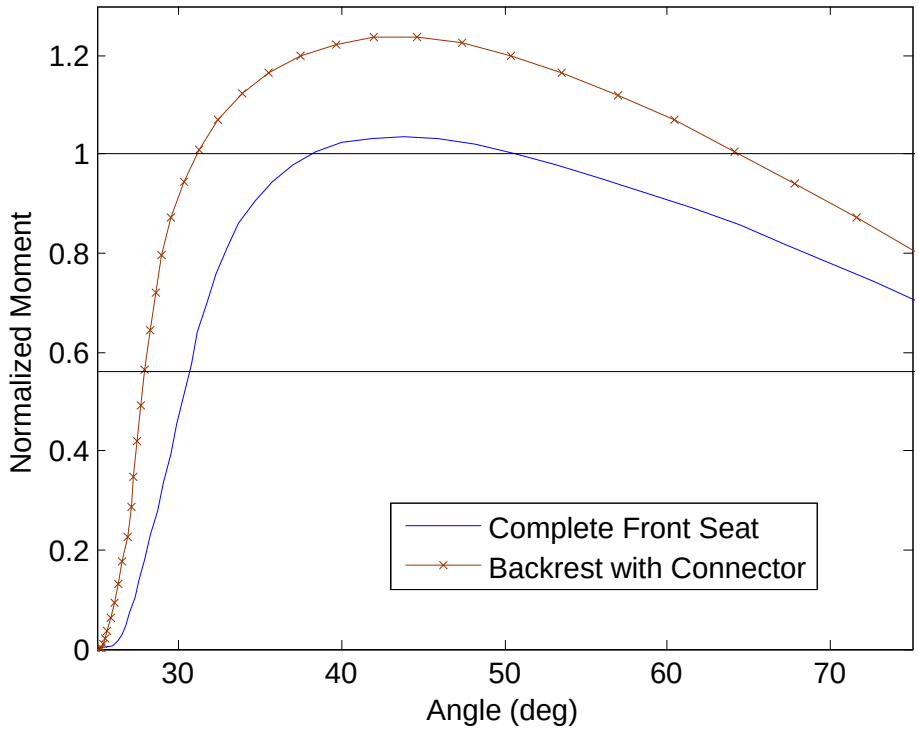

Figure 6-7: Moment Deflection Plots of Reference front Seat with and without Base Frame for Moment Test (Constant Horizontal Force)

6.4 Simulation of Moment Test (Constant Horizontal Force) without Base frame and Connector

In this section, the moment test is simulated using a constant horizontal force is simulated with the backrest isolated from the connector and base frame in order to understand the strength and deflection performance of backrest and effects of base frame and connector stiffness on moment deflection characteristics. The backrest is locked by constraining the bearing surfaces of the sleeve pocket in the rearward direction. Multi-point constraints are created using rigid links to represent bolts connections at the location where the connector is bolted to the sleeve pocket of

the backrest. The centers of the circular edges of bolt holes are constrained except for the rotation about the axis connecting the centers of pivot points.

When considering the component backrest frame restrained at the bearing surfaces of the sleeve pocket, the high stress values developed as shown in Figure 6-8 during the moment test on the backrest occurred on the vertical members where the transitions from wide at the bottom to narrow at the top and on the region surrounding the sleeve pocket. The high stress of 365 MPa located on the backrest is well above the yield point of 305 MPa, but below the ultimate strength of 430 MPa for low strength steel.

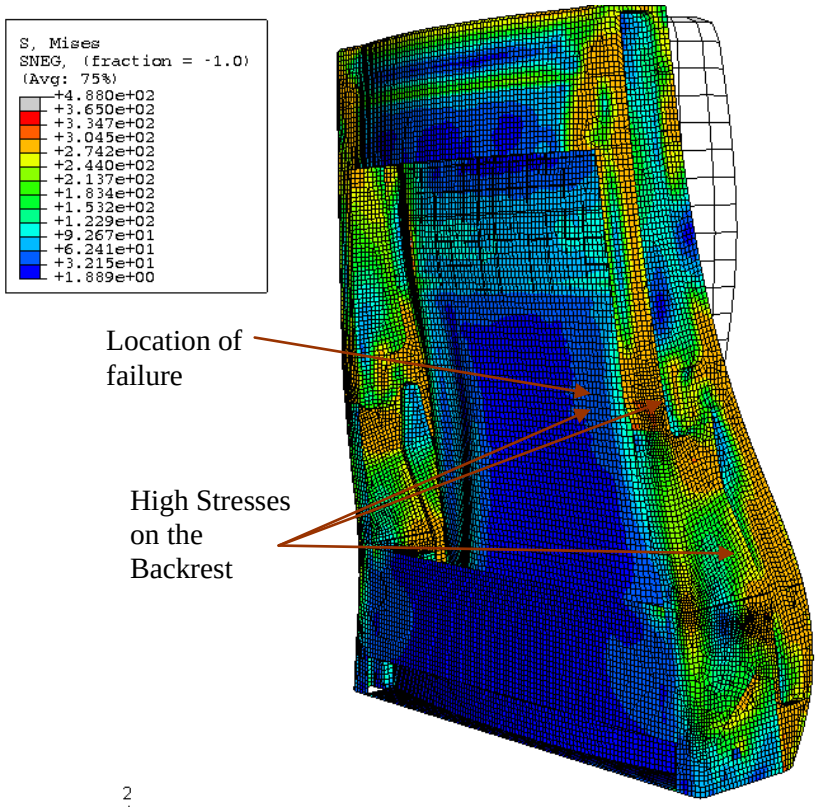

Figure 6-8: Contours of Von Mises Stress on Reference Seat Backrest Component for Moment Test (Constant Horizontal Force)

The component backrest model without base frame and connector withstands a maximum normalized moment of 1.2 through a deformation angle of 5 degrees as shown in Figure 6-9. After the deformation angle of 5 degrees, the vertical members of the backrest buckle due to reduced stiffness under high stress at the location where it transitions from wide at the bottom to narrow at the top.

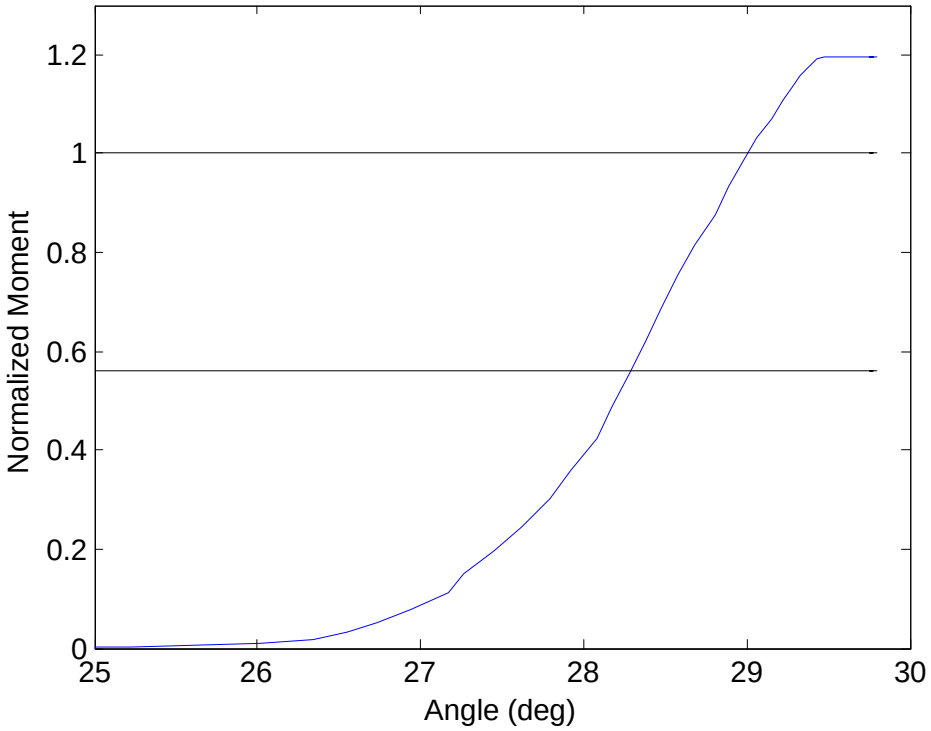

Figure 6-9: Moment Deflection Plots of Reference Seat Backrest without Connector and Base Frame for Moment Test (Constant Horizontal Force)

6.5 Influence of Plastic Material Properties on Strength

This section, discusses the simulation of the moment test using the constant horizontal force is discussed on the full scale reference seat with different ultimate and yield strength values of steel used for different load bearing components is examined in order to understand the

influence of material properties on moment deflection characteristics. The moment deflection characteristics of the reference complete seat model with low strength steel (yield strength 305 MPa, ultimate strength 365 MPa) for backrest, medium strength steel (yield strength 350 MPa, ultimate strength 515 MPa) for base frame and high strength steel (yield strength 365 MPa, ultimate strength 635 MPa) for connector were obtained earlier Section 6.1.

For comparison the moment test using constant horizontal force is simulated on a seat model with medium strength steel for backrest, base frame and high strength steel for connector. For this material distribution, the highest stress values developed on the backrest is 345 MPa which is below the yield value of 350 MPa for medium strength steel, and is located on the vertical members where the cross-section transitions from wide at the bottom to narrow at the top and side bolster region of the backrest as shown in Figure 6-10. The backrest base frame connector has a maximum stress of 570 MPa well above the yield value of 365 MPa and below the ultimate strength of 687.4 MPa for high strength steel. High stresses of 390MPa on the base frame are located near the pivot point. The high stress on the base frame is above the yield value of 350 MPa for medium strength steel.

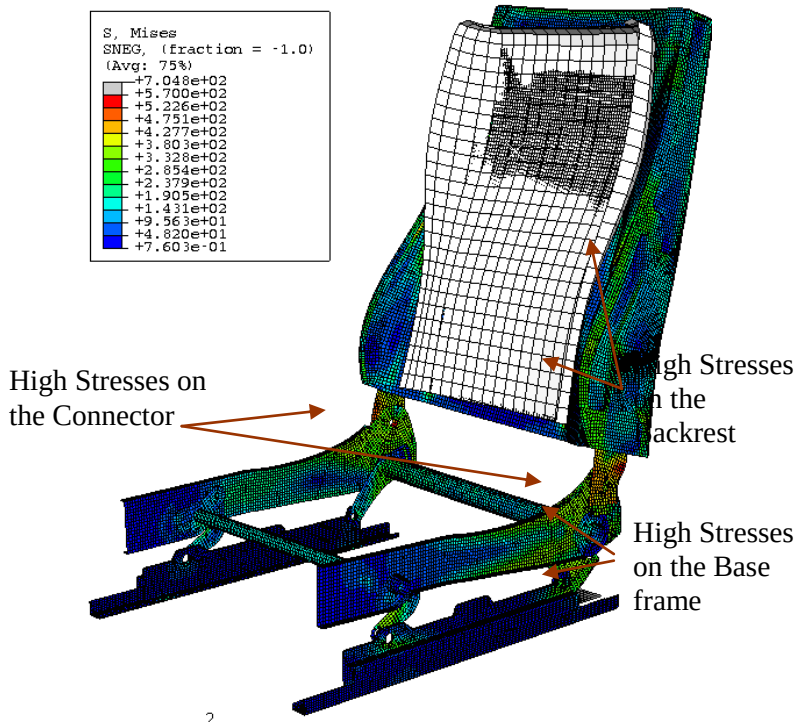

Figure 6-10: Contours of Von Mises Stress on Seat with medium strength steel for backrest, base frame and high strength steel for connector in a Moment Test (Constant Horizontal Force)

For further comparison, the moment test using constant horizontal force is simulated on a seat model with medium strength steel for backrest, base frame and connector. The highest stresses value developed during moment test on the backrest are located on the vertical members where the cross-sections transition from wide at the bottom to narrow at the top and side bolster region of the backrest. The high stress of 345 MPa on the backrest is below the yield of value of 350 MPa for medium strength steel as shown in Figure 6-11. The backrest base frame connector has a maximum stress of 530MPa well beyond the yield value of 350 MPa and below the ultimate strength of 580 MPa for medium strength steel. High stresses of 365 MPa on the base frame are located near the pivot point. The high stress on the base frame is above the yield value of 350 MPa for medium strength steel.

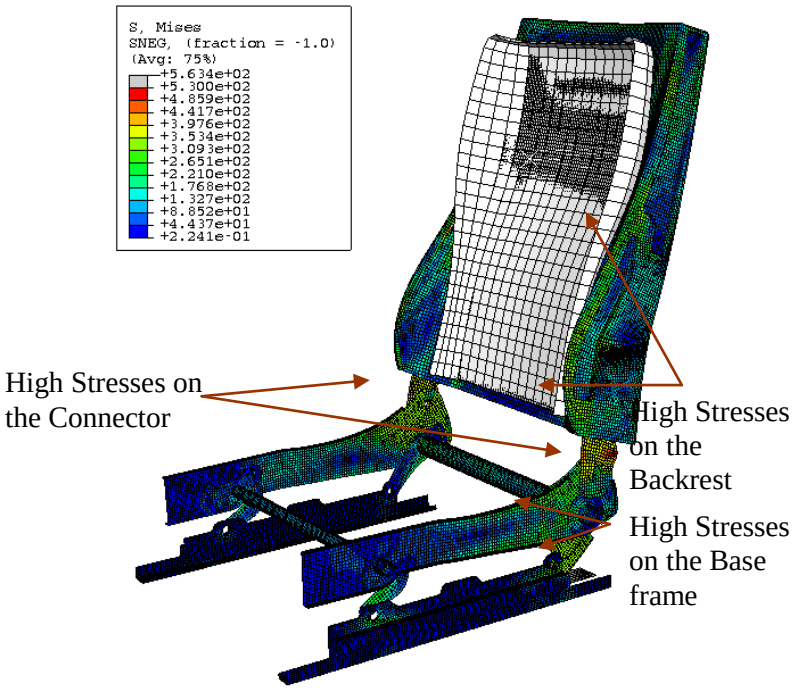

Figure 6-11 Contours of Von Mises Stress on Seat with medium strength steel for backrest, base frame and connector in a Moment Test (Constant Horizontal Force)

The three seat models simulated with different plastic properties meet the requirements by withstanding a normalized moment of 1 up to an intermediate angle and remains above 0.56 until the end of the deformation path as shown in Figure 6-12. The seat with medium strength steel backrest, base frame and high strength steel backrest withstand higher moment than the seat with low strength steel backrest, medium strength steel base frame and high strength steel connector. The seat with medium strength steel backrest, base frame and connector has similar moment deflection characteristics compared to the seat with low strength steel backrest, medium strength steel base frame and high strength steel connector. The initial strength and deflection characteristics for all the models are same because the different grades of steel used have the same elastic properties.

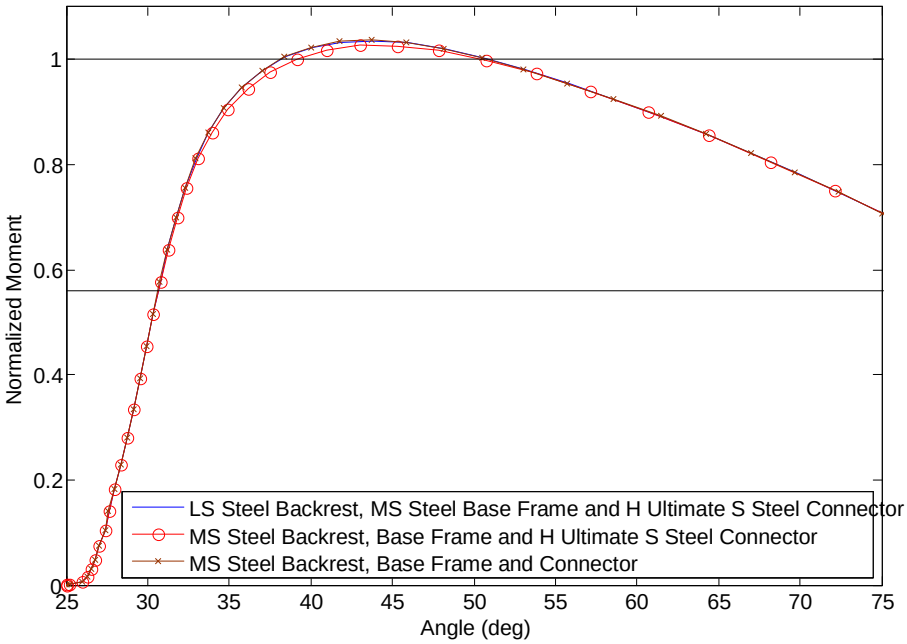

Figure 6-12: Moment Deflection Characteristics for Various Strengths of Steel Used for Modeling the Seat.

In order to understand the effect of increase in the yield point of steel on the major load bearing components, a moment test using constant horizontal force is simulated on a seat model with medium strength steel for base frame, low strength steel for backrest and high yield strength steel (yield strength 495 MPa, ultimate strength 640 MPa and ductility 10%) for the connector are used. The highest stresses value developed during moment test on the backrest are located on the vertical members where the cross-sections transition from wide at the bottom to narrow at the top and side bolster region of the backrest. The high stress of 325 MPa on the backrest is above the yield of value of 305 MPa for medium strength steel. The backrest base frame connector has a maximum stress of 585 MPa well beyond the yield value of 495 MPa and below the ultimate strength of 704 MPa for high yield strength strength steel. High stresses of 365 MPa on the base frame are located near the pivot point. The high stress on the base frame is above the yield value

of 350 MPa for medium strength steel. The failure on the seat model occurred on the side flanges by buckling towards the end of the deformation path.

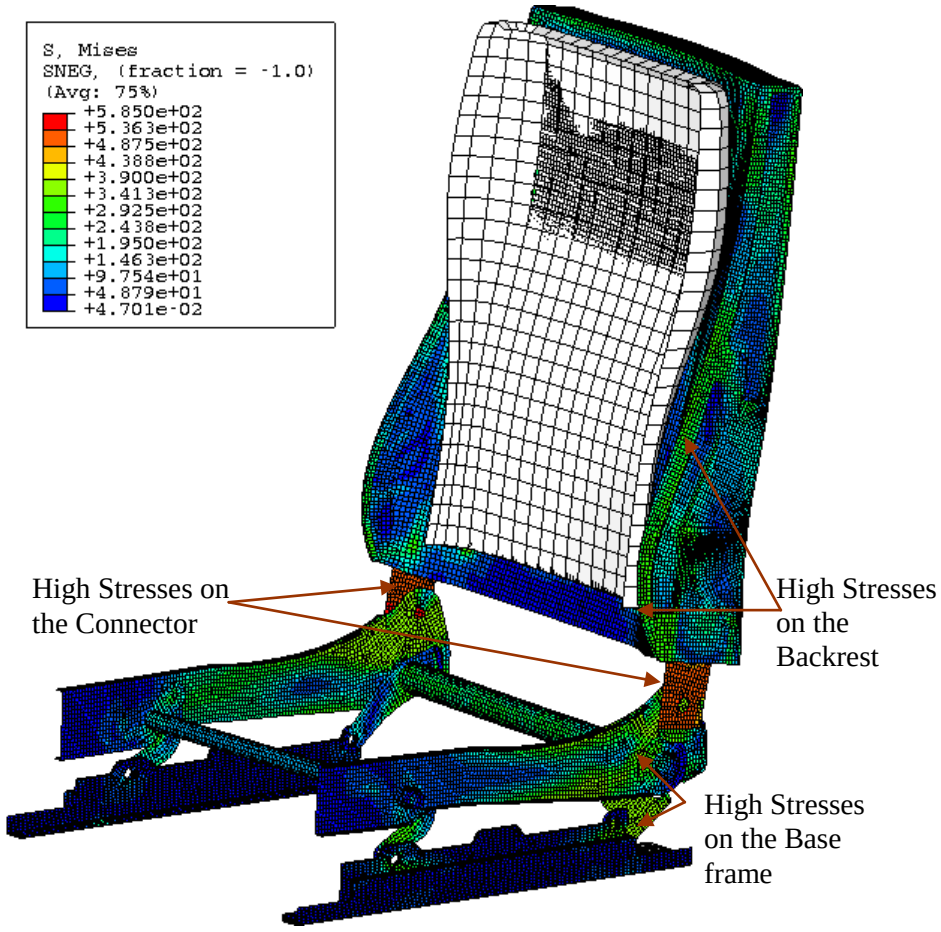

Figure 6-13: Contours of Von Mises Stress on Seat with medium strength steel for backrest, low strength steel for base frame and high yield strength steel for connector in a Moment Test (Constant Horizontal Force)

Figure 6-14 shows the maximum in-plane principal plastic strain in the reference seat model. The maximum principal plastic strain of 0.005 in the backrest is located on the transition region from wide at the bottom to narrow at the top and surrounding the connector pocket sleeve.

The maximum stain of 0.02 in the base frame is located on the door side leg and pivot point region. The maximum strain in the connector is 0.06.

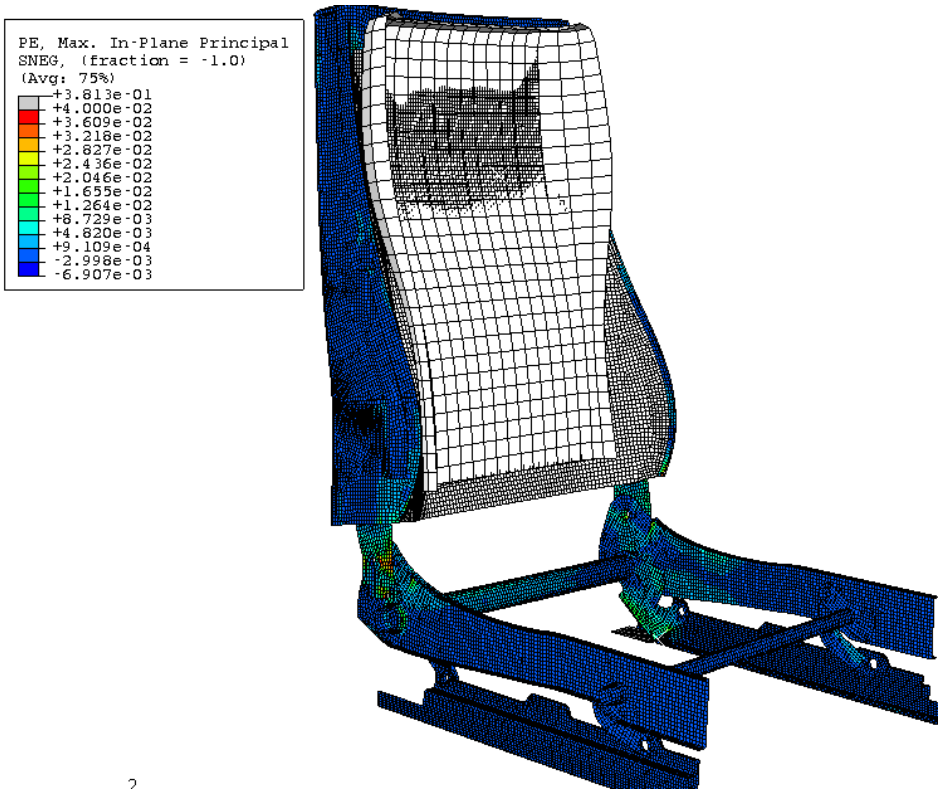

Figure 6-14: Contours of Plastic Strain in the Reference Seat Model

The seat model simulated with high yield strength steel properties meet the requirements by withstanding a normalized moment higher than 1 until 50 degrees torso angle and maintains above 0.56 until the end of the deformation path. The seat withstands a higher moment than the seat with low strength steel backrest, medium strength steel base frame and high ultimate strength steel connector.

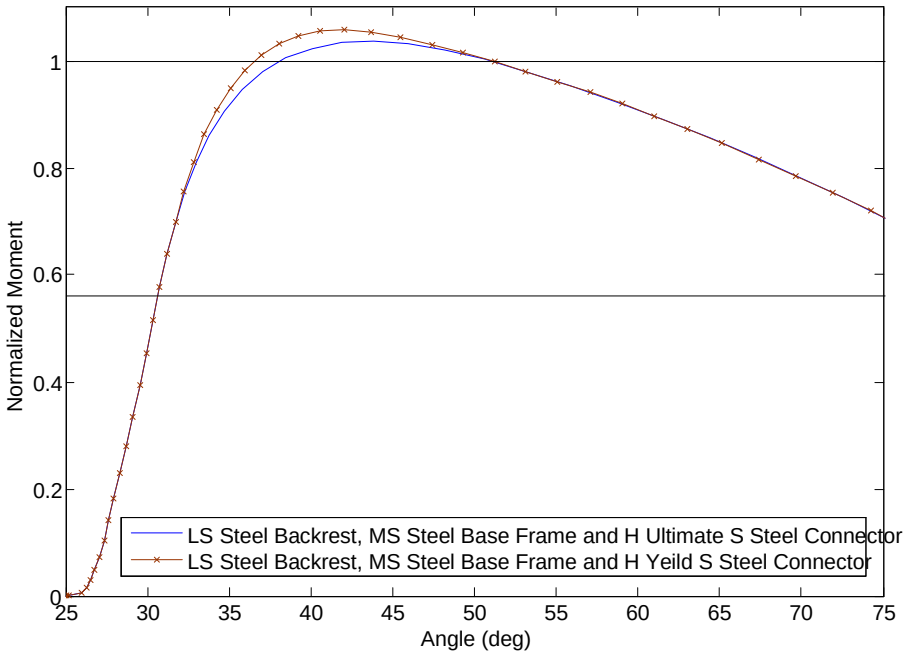

Figure 6-15: Moment Deflection Plots for Different Yield Strength Steels Used for Modeling the Seat.

6.6 Influence of Length of Pivot Arm of Body Form on Moment Deflection Characteristics

The length of the pivot arm connecting the reference point of the body form and the H-point in a moment test using constant horizontal force is increased by moving the reference point of the body form towards the upper portion of the body form. The length of the pivot arm connecting the H-point and the reference point is increased from the initial value of 360 mm to 440 mm above the H-point. The force F applied at the reference point in the horizontal direction is modified to create an initial moment of $M_1 = Fd_1 = 1.12M_0$ N-m about the H-point of the seat at initial position. The force applied on the reference point of the body form causes the body form to initially contact the front mesh and the backrest top cross member. The body form is free to

rotate about the reference point so after a short amount of time establishes contact at the top region of the front mesh because of change in the location of reference point to upper portion of the body form. The highest stress values developed during the moment test on the backrest are located where the vertical members transition from wide at the bottom to narrow at the top because the body form applies a pressure load over the top region of front mesh. The high stress of 310 MPa on the backrest is slightly beyond the yield of value of 305 MPa for low strength steel. The backrest base frame connector has a maximum stress of 560 MPa well beyond the yield value of 365 MPa yet below the true failure value of 787.4 MPa for high strength steel The load transferred to the pivot point of the side flanges from the connectors causes a high stress of 410 MPa surrounding the pivot point, which is beyond the yield value of 350 MPa of medium strength steel used for the base frame.

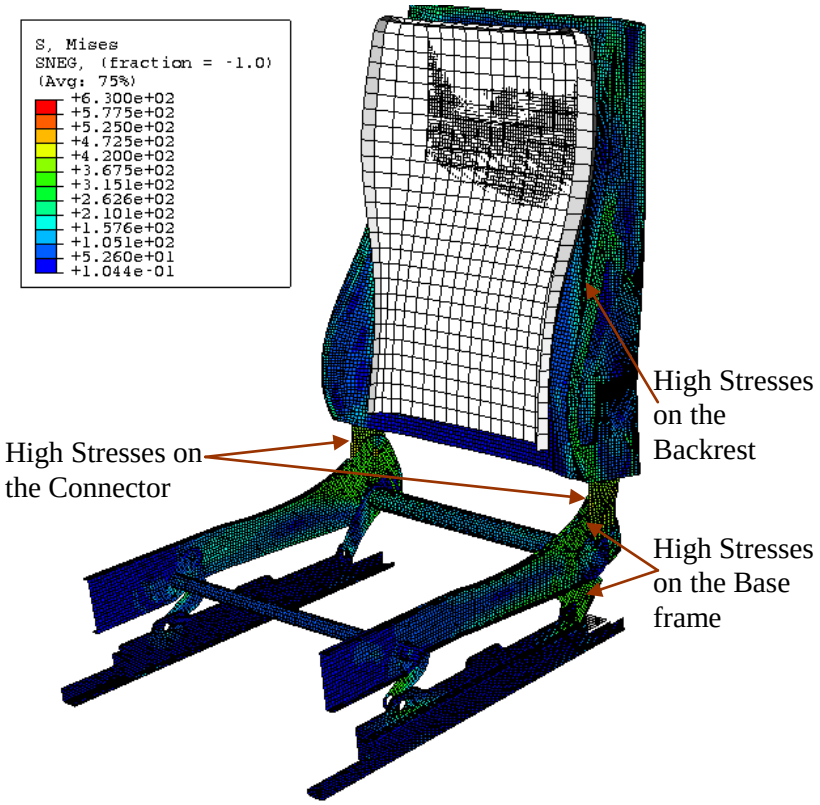

Figure 6-16 Contours of Von Mises Stress on Reference Front seat with Modified Distance between H-point and Reference Point for Moment Test (Constant Horizontal Force)

Figure 6-17 shows the developed moment about the H-point versus change in torso angle Results from the simulation show that, the reference front seat with the pivot arm length increased withstands a normalized moment of 1 at an intermediate torso angle and maintains above 0.56 at the final angle considered. The moment deflection characteristic of the seat with pivot arm length increased to 430 mm withstands higher moment initially because the effective moment developed due to the load acting on the upper portion of the backrest is greater when compared to the 360 mm original length of the pivot arm. The body form with 360mm pivot arm length loads the connector in the lateral direction as the body form contacts uniformly over the entire front mesh region loading the lower portion of the vertical members in the lateral direction, whereas the body form with 430mm pivot arm length contacts more on the top region of the front mesh eliminating

lateral loads on the lower portion of vertical members. Towards the end of the deformation path the seat maintained above a lower moment with the pivot arm length increased because the body form contacts the upper portion of the backrest

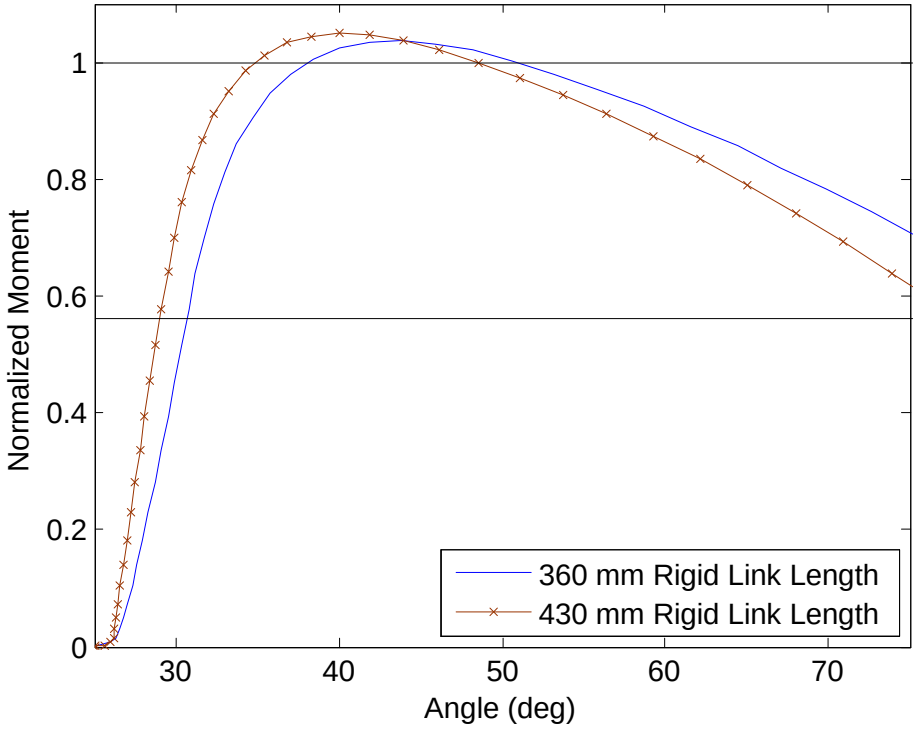

Figure 6-17 Moment Deflection Plots for Reference Front seat with 360 mm and 430 mm Distance between H-point and Reference Point for Moment Test (Constant Horizontal Force)

6.7 Influence of Body Form Rotation about Reference Point on Moment Deflection Characteristics

In this section, moment test using constant horizontal force is simulated by constraining the rotation of the body form about reference point axis. The body form along with the pivot arm is free to rotate about the H-point. The body form rotation about reference point axis is

constrained by attaching a rigid link which will constrain all degrees of freedom of reference point to the H-point. The horizontal force applied at the reference point of the body form causes the body form to contact the top portion of the backrest as the body form is not allowed to rotate about the reference point axis. The highest stress values developed during the moment test on the backrest are located on the vertical members where the cross-sections transition from wide at the bottom to narrow at the top because the body form contacts the upper portion of the backrest. The high stress of 300 MPa on the backrest is less than the yield value of 310 MPa. Figure 6-18 shows contours of Von-Mises stress when moment about the H-point reaches a maximum value. The backrest base frame connector has a maximum stress of 580 MPa well beyond the yield value of 365 MPa yet below the true failure value of 787.4 MPa for high strength steel. The load transferred to the pivot point of the side flanges from the connectors causes a high stress of 380 MPa surrounding the pivot point, which is beyond the yield point of medium strength steel used for the base frame.

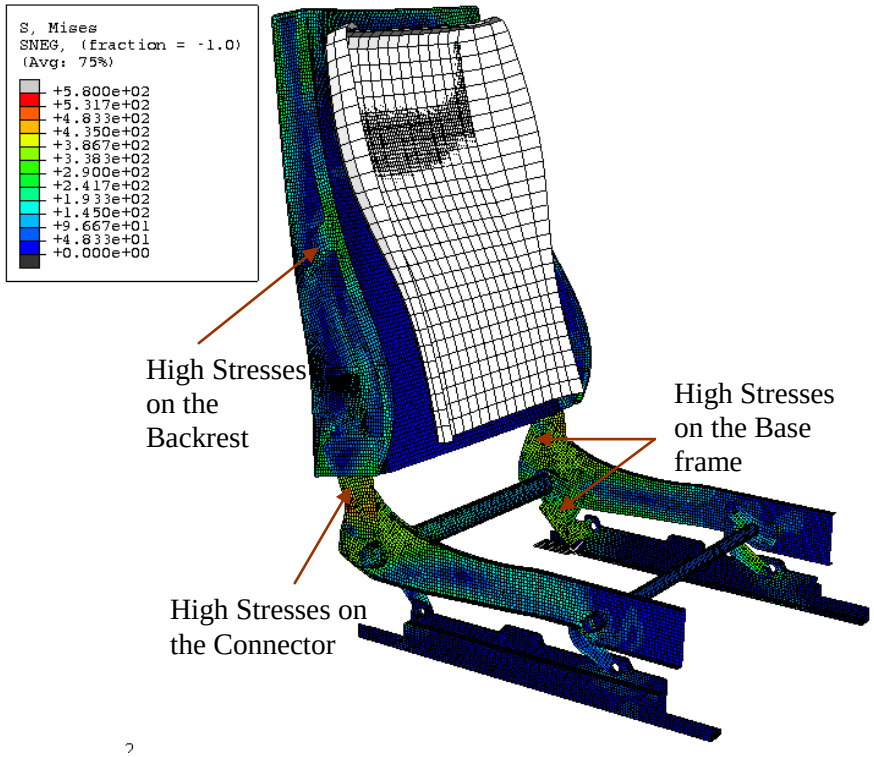

Figure 6-18: Contours of Von Mises Stress on Reference Front Seat with Body Form Rotation about Reference Point Axis Constrained for Moment Test (Constant Horizontal Force)

Figure 6-19 shows the developed moment about the H-point versus change in torso angle. Results from the simulation show that, the moment test on the reference front seat with rotation of the body form constrained about the reference point axis withstands a normalized moment of 1 at an intermediate angle and maintains above 0.56 at the final torso angle considered. The seat withstands higher moment initially with the rotation of the body form constrained because the load acts only on the top portion of the backrest creating higher effective moment about the pivot point. The body form with rotation about the reference point loads the connector in the lateral direction as the body form contacts uniformly over the entire front mesh region loading the lower portion of the vertical members in the lateral direction, whereas the body form with rotation

constrained about the reference point contacts only the top region of the front mesh with no lateral loads on the lower portion of vertical members and the connector.

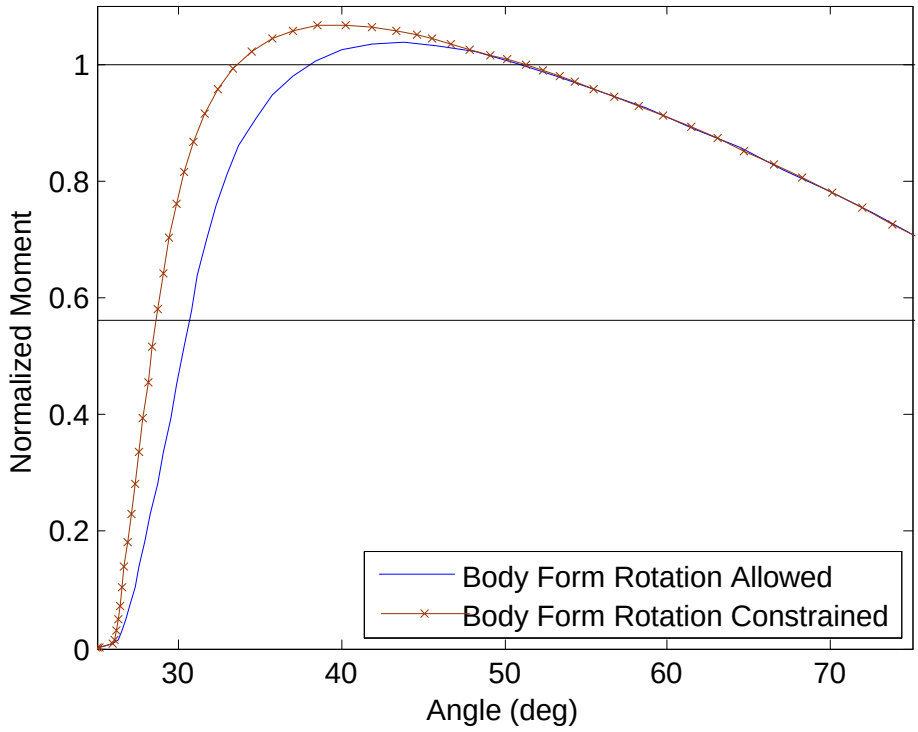

Figure 6-19: Moment Deflection Characteristics of Reference Front Seat with Body Form Rotation about Reference Point Axis Free and Constrained for Moment Test (Constant Horizontal Force)

6.8 Influence of Backrest Mesh Contour on Moment Deflection Characteristics

In this section, the moment test using constant horizontal force is simulated using the reference seat model without front mesh contour on the backrest. The front mesh contour is modified by creating a mesh surface formed by sweeping the top cross member edge along the front edge of vertical members. The body form is positioned in front of the front mesh surface so that the reference point of the body form coincides with the H-point of the seat.

Figure 6-20: Front Mesh on the Backrest without Contour

The horizontal force applied at the reference point of the body form causes the body form to contact the lower portion of the backrest creating a lateral load on the side bolster region of the vertical members and the connectors. Figure 6-21 shows contours of Von-Mises stress when moment about the H-point reaches a maximum value. The highest stress values developed during the moment test on the backrest are located on the side bolster region of the vertical members because of the lateral loading on the lower portion of the backrest. The high stress of 315 MPa on the backrest slightly above the yield value of 310 MPa. The backrest base frame connector has a maximum stress of 570 MPa well beyond the yield value of 365 MPa yet below the true failure value of 787.4 MPa for high strength steel. The load transferred to the pivot point of the side

flanges from the connectors causes a high stress of 410 MPa surrounding the pivot point, which is beyond the yield point of 350 MPa for medium strength steel used for the base frame.

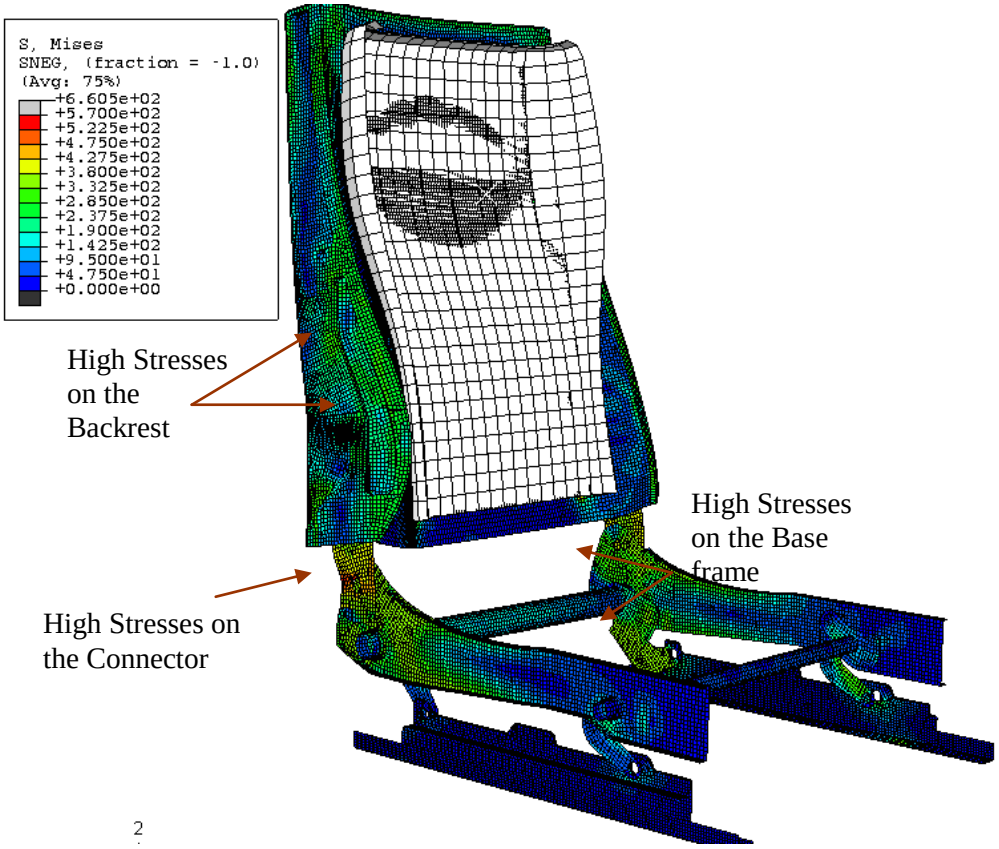

Figure 6-21: Contours of Von Mises Stress on Reference Front Seat with front mesh with no contour for Moment Test (Constant Horizontal Force)

Figure 6-22 shows the developed moment about the H-point versus change in torso angle. Results from the simulation show that seat model with modified front mesh without contour on the backrest does not withstand a normalized moment of 1 at an intermediate angle but maintains the required normalized moment 0.56 at the final torso angle considered. The seat without front mesh contour withstands a moment less than the seat with front mesh contour because of the

lateral load acting on the vertical members deforms the vertical members near the side bolster region inward.

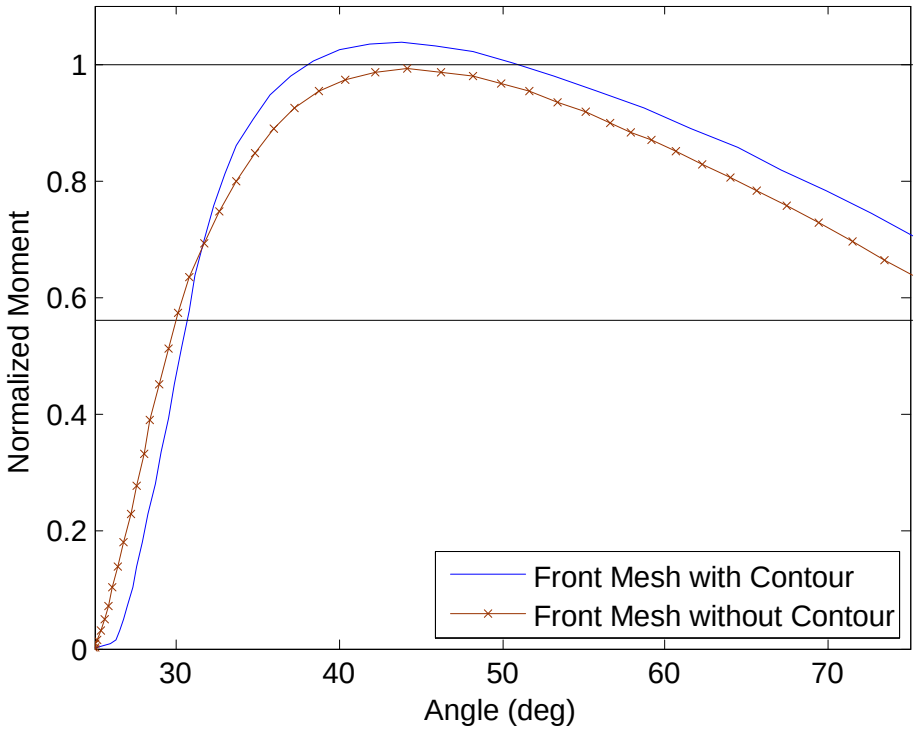

Figure 6-22: Moment Deflection Plots for Reference Front Seat with Original and Modified Front Mesh Contour For Moment Test (Constant Horizontal Force)

6.9 Influence of Weld Connection between Connector and Backrest on Moment Deflection Characteristics

In this section, the moment test using constant horizontal force is simulated on the reference seat by attaching the connector directly to the inner surface of the sleeve pocket. The backrest base frame connector is welded to the sleeve pocket, eliminating the bearing contact between connector and backrest sleeve pocket. The connector is moved inline and attached to the

support structure forming the pocket sleeve on the lower portion of the backrest as shown in Figure 6-23.

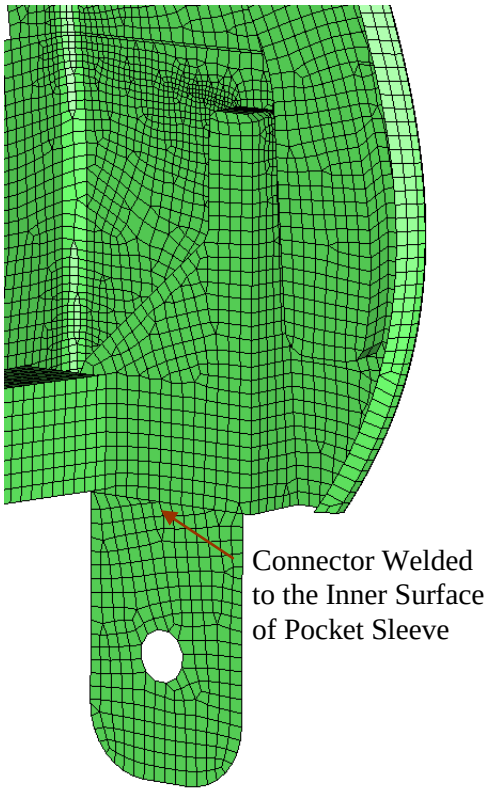

Figure 6-23: Connector Welded to the Sleeve Pocket

The highest stress values developed during the moment test on the backrest are located where the vertical members transition from wide at the bottom to narrow at the top and on the side bolster of the vertical members. The high stress of 320 MPa on the backrest is beyond the yield of value of 305 MPa for low strength steel. The backrest base frame connector has a maximum stress of 541 MPa well beyond the yield value of 365 MPa yet below the true failure value of 787.4 MPa for high strength steel The load transferred to the pivot point of the side

flanges from the connectors causes a high stress of 410 MPa surrounding the pivot point, which is beyond the yield value of 350 MPa of medium strength steel used for the base frame

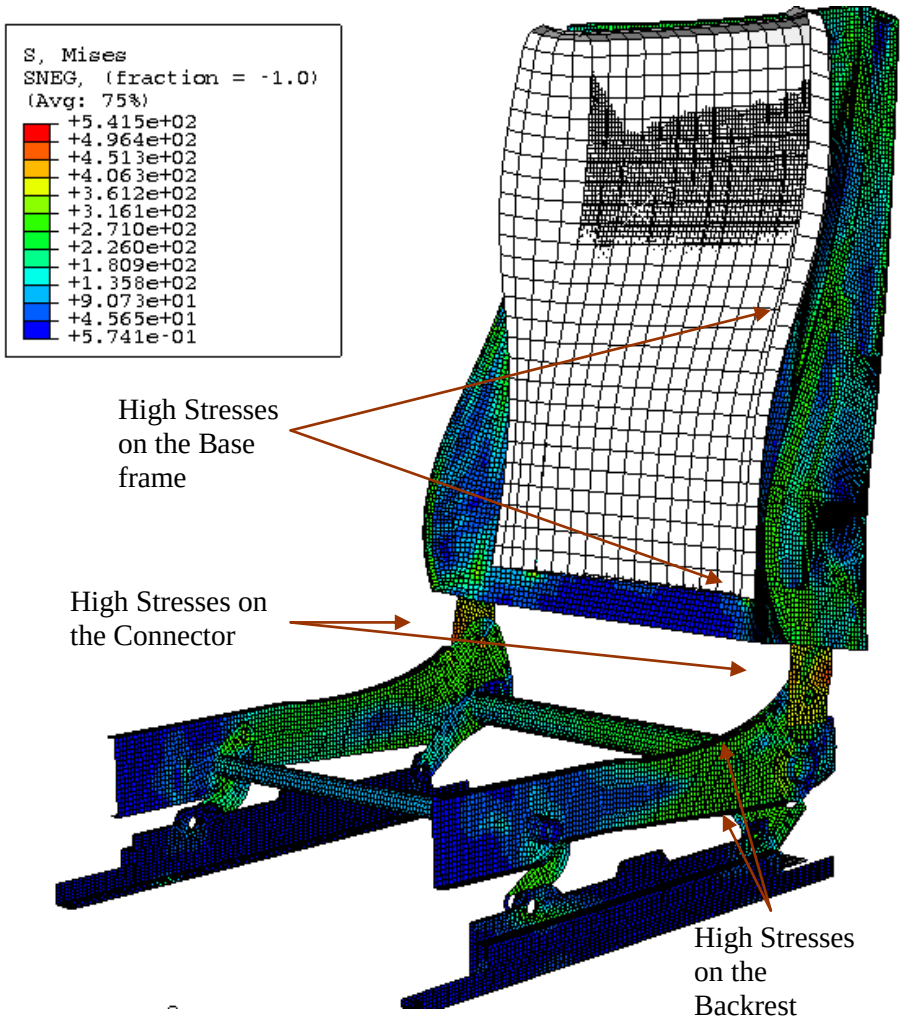

Figure 6-24: Contours of Von Mises Stress on Reference Front Seat with Connector Welded to Sleeve Pocket for Moment Test (Constant Horizontal Force)

Figure 6-25 shows the developed moment about the H-point versus change in torso angle. Results from the simulation show that, the seat model with connector welded to the support structure of the vertical members forming the sleeve pocket withstands a normalized moment of 1

at an intermediate torso angle and maintains above 0.56 towards the end of the deformation path. The seat model with connector welded to the backrest is stiffer and withstands a higher moment than the reference seat model because of the modification of attachment between the connector and backrest.

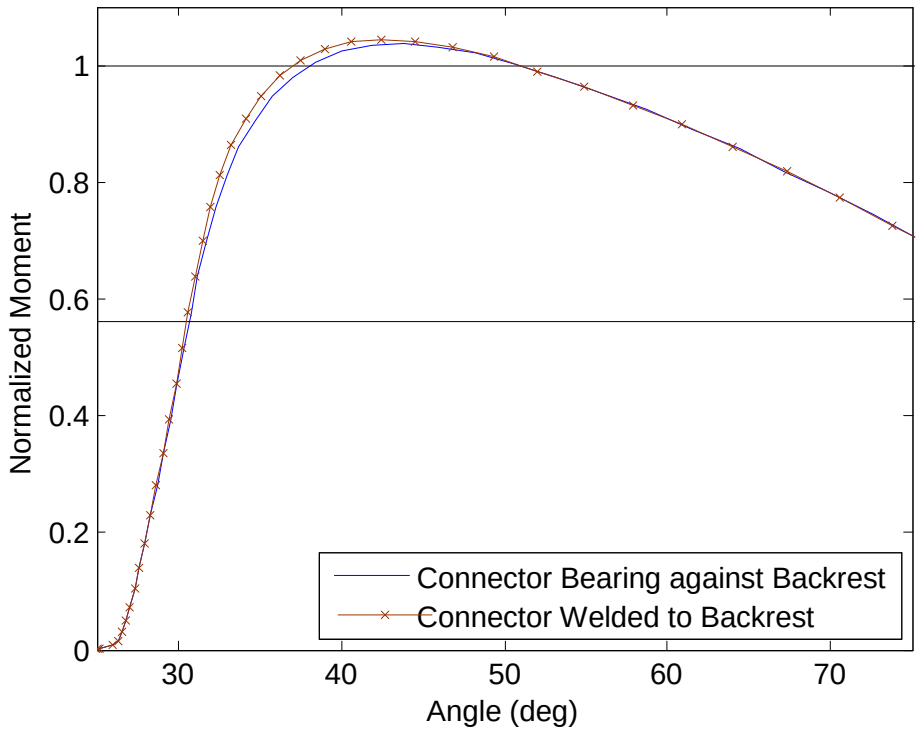

Figure 6-25: Moment Deflection Plots of Reference Front Seat with Connector Welded to Sleeve Pocket and connector bearing against sleeve pocket for Moment Test (Constant Horizontal Force)

CHAPTER 7

CONCLUSION

The reference seat is analyzed beyond the component level by using a complete seat model formed by integrating the major structural components including the base frame, slider rails, and backrest. The moment deflection characteristics of the reference seat, obtained by simulating the moment test using two complementary loading cases (constant horizontal force and constant angular velocity) in accordance with ECE R17, meet the requirements for strength in an event of vehicle rear impact.

Since the ECE R17 regulations do not provide precise specifications for the height of the applied force and test setup for the body form pivot mechanism, a study is conducted in order to understand the influence of body form rotation and height of the body form above the H-point. The influence of plastic material properties of different grades of steel used for the seat model, front mesh contour on the backrest and connection between the backrest and connector are modified to analyze the influence of load path on moment deflection characteristics of a seat.

The moment test setup simulated with increased length of the pivot arm of 430 mm shows higher strength for initial deflection and lower strength towards the end of the deformation path when compared to original length of 360mm. The moment test setup, simulated with body form rotation about the reference point axis constrained shows higher strength for initial deflection and similar strength towards the end of the deformation path when compared to free rotation of the body form about reference point axis.

The front mesh without contour on the backrest decreases the strength of the seat below the requirement. The welded connections between the backrest base frame connector and sleeve pocket of the backrest showed a small improvement in moment deflection characteristics at the intermediate angle of the deflection path and similar strength towards the end of the deformation

path when compared to a bearing contact between the connector and sleeve pocket of the backrest.

Different grades of ductile steel were considered. Each grade had the same elastic properties. Changing the ultimate strength of steel used on the major load bearing components does change the component stress, but had only a small change in the moment deflection characteristics of the model. The low strength steel (yield strength 305 MPa, ultimate strength 365 MPa) on the backrest does not influence the moment deflection characteristics of the seat and the model shows similar performance when medium strength steel (yield strength 350 MPa, ultimate strength 515 MPa) is used. The connector with high strength steel (yield strength 365 MPa, ultimate strength 635 MPa) showed slightly improved strength when compared to medium strength steel (yield strength 350 MPa, ultimate strength 515 MPa). Using a high yield strength steel material (yield strength 475 MPa, ultimate 635 MPa) for the connector increases the maximum moment supported by a small amount.

In order to study the effects of assuming a rigid base frame, the backrest and connector are isolated from the base frame. The moment test with a magnitude several times larger than the ECE requirement is simulated on the backrest with connector model restrained at the interface with the base frame, and withstands a higher moment compared to the complete seat model. The moment test is also simulated on the component backrest isolated from the connector and base frame, and withstands a higher moment for small torso angle deformation less than 5 degrees compared to the complete seat model. After reaching its maximum moment, the component backrest model restrained at the bearing surfaces of the sleeve pocket buckled due to reduced stiffness on the back side of the vertical members near the transition from wide at the bottom to narrow at the top.

7.1 Future Work

In this section, some directions for future research work extending this thesis are identified.

- Include detailed models of the cams and locking gears for height adjustment, front tilt adjustment, and backrest tilt adjustment mechanisms. This would require a hybrid finite element model which models the cams and gears with solid elements attached to the shell elements modeling the stamped sheet of the base frame side flanges. Detailed contact models between the locking meshes would be needed together with rotation around detailed solid pins. Studies comparing these detailed locking models to the rigid link models considered in this work could be performed.
- Simulate other tests for seat components such as the sled test and seat belt test [18] in accordance with government regulations on the reference automotive front seat. The vehicle rear impact test studied in this work is the primary load case which drives the design for strength of the backrest and connectors, and also produces large forces in the base frame and slider rails. Simulation of the seat belt test would require modeling contact between lap and torso rigid body forms [19] described in ECE R14 with seat belts and tensioners. By simulating the seat belt test, a better understanding of the strength performance of the base frame, slider rails, and seat belt connector brackets for frontal impact would be obtained.
- Replace the polymeric mesh model for the resting surface of the backrest with detailed PUR foam and fabric cover material model. This would require a complex geometry representation of the detailed contours in the foam surface and clamped conditions to the backrest frame. Some models for PUR foam materials are reported in [20].

REFERENCES

1. Consolazio, G.R., J.H. Chung, and K.R. Gurley, "Impact simulation and full scale crash testing of a low profile concrete work zone barrier". Computers & Structures, 2003. 81(13): p. 1359-1374.

2. Chen, C.J. and M. Usman, "Design optimisation for automotive applications". International Journal of Vehicle Design, 2001. 25(1): p. 126-141.

3. ECE-R17 UNECE Agreement Concerning the Adoption of Uniform Technical Prescriptions for Wheeled Vehicles, Uniform Provisions Concerning the Approval of Vehicles with Regard to the Seats, their Anchorages and Any Head Restraints.

4. FMVSS NO. 202 Head Restraints for Passenger Vehicles, Office of Regulatory Analysis and Evaluation Plans and Policy, December 2000.

5. Molino, L., "Determination of Moment-Deflection Characteristics of Automobile Seat Backs". 1998, NHTSA Technical Report, DOT Docket Management Systems. NHTSA-1998-4064.

6. Viano, D. C., 2004, “High Retention Seat Performance in Quasistatic Seat Tests,” in Recent Developments in Automotive Safety Technology, Edited by Daniel J. Holt, SAE International, Paper Number 2003-01-0173, pp. 123-135.

7. Timothy N. MacNaughtan and Shafiq R. Khan, "Correlation of an Automotive Seat Finite Element Simulation with Dynamic Sled Testing". 2005 SAE World Congress, Paper Number 2005-01-1301.

8. Hesser, D.S., "Integration of finite element method to enhance modeling and analysis for reverse engineering". M.S. Thesis, Clemson University, 2006.

9. Hesser, D. S., and Thompson, L., November, 2005. “Finite Element Analysis of the Strength and Deflection of a Seat Backrest Frame”, Technical Report, Department of Mechanical Engineering, Clemson University.

10. Carol A. C. Flannagan, "Reproducibility and Repeatability of the SAE J4002 and J826 H-point Machines". SAE Technical Paper Series, 2005. Human Factors in Driving, Telematics, and Seating Comfort 2005 (SP-1934).

11. Helen A. Kaleto and Michael J. Worthington, "Proposed Upgrade to Federal Motor Vehicle Safety Standard (FMVSS) 202 – Head Restraints:Methodology and Equipment". 2004.

12. T.D.S Solutions, BIA Head & Seat Back Restraint Testing Rig. Automotive Testing Expo Europe 2006.

13. Hibbeler, R.C., Mechanics of Materials. Prentice Hall, 2000.

14. DASSAULT SYSTEMES, Simulia, D., ABAQUS Analysis User's Manual. ABAQUS v6.6 Documentation.

15. DASSAULT SYSTEMES, Simulia, Getting Started With ABAQUS/Standard. ABAQUS Documentation V6.6.

16. DASSAULT SYSTEMES, Simulia, ABAQUS Theory Manual. ABAQUS v6.6 Documentation.

17. "Automobile Roof Crush Analysis with Abaqus". Abaqus Technology Brief, April 2007.

18. I-DEAS 11 NX Series m2, 2004, UGS Corp.

19. M. Grujicic and J. Hodges, "A finite element analysis of the functional performance of the Mercedes SLK automotive seat backrest frame", Technical Report, Department of Mechanical Engineering, Clemson University, October, 2005.